Yucca Mountain

Looking ten thousand years into the future

by Roger C Eckhardt
for David L. Bish, Gilles Y. Bussod, June T. Fabryka-Martin, Schön S. Levy, Paul W. Reimus, Bruce A. Robinson, Wolfgang H. Runde, Inés Triay, and David T. Vaniman

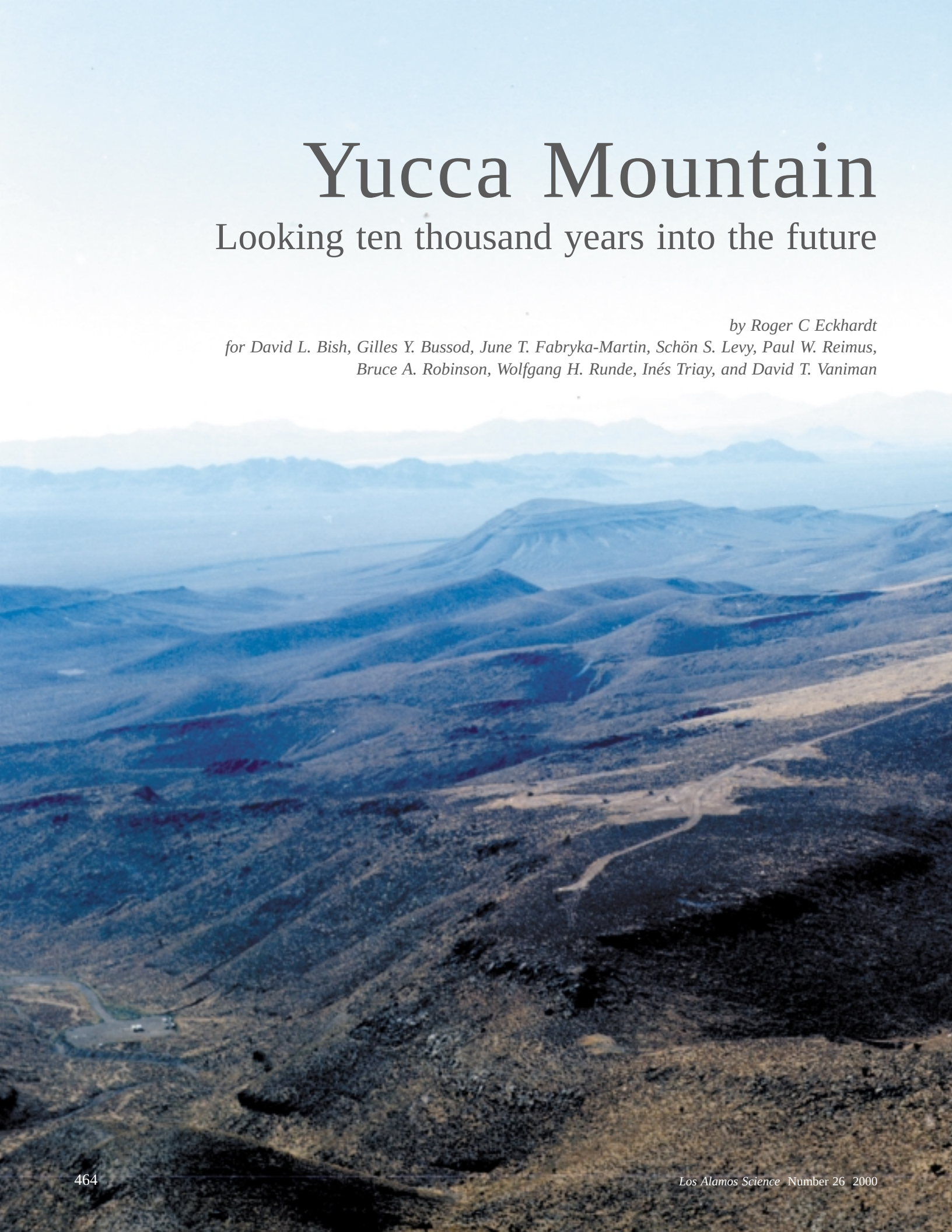

It's a dry, brown, nondescript ridge near the Amargosa Desert, just north of Death Valley and west of the Nevada Test Site. The landscape is a drab mix of desert grasses, cacti, shrubs—like needleleaf rabbitbrush and Cooper goldenbush—and, of course, the occasional Yucca plant. Nothing moves but scrawny black-tailed jackrabbits and desert collared lizards. No man's land.

Yet for the past twenty years, the ridge—called Yucca Mountain but looking more like a geologic speed bump—has been scrambled over by geologists, hydrologists, volcanologists, engineers, and environmental scientists. It has been photographed from every angle and cored at hundreds of drill sites to characterize its geology and hydrology. Its plant and animal life has been cataloged, its topography charted, and its underlying volcanic tuff captured in three-dimensional computer grids.

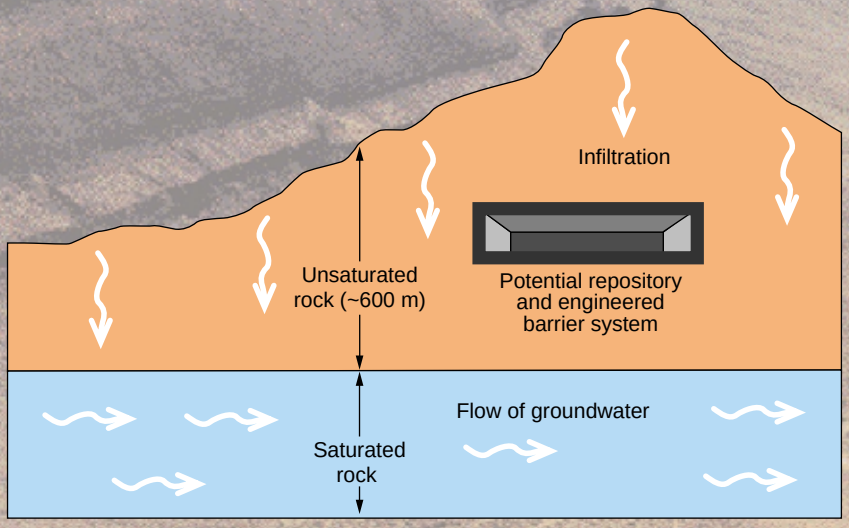

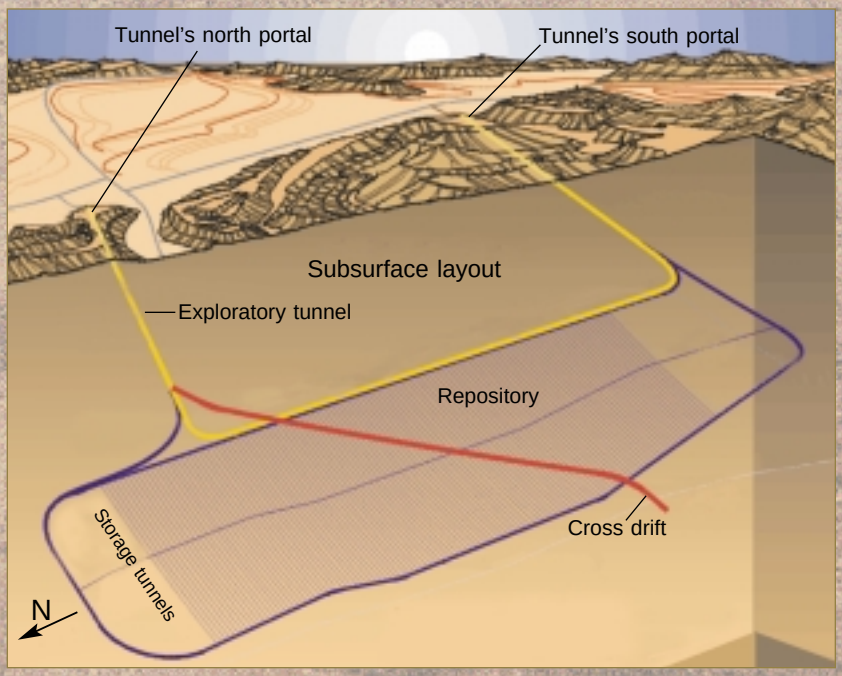

Figure 1. Potential Yucca Mountain Repository Site

Yucca Mountain's remote desert location and deep water table make it attractive as a potential burial site for high-level nuclear waste. The nearest community is in Amargosa Valley, 30 km away. (Top) The water table is among the deepest in the world, which allows building a repository that is both deep underground and yet well above the water table. (Bottom) The proposed repository with its rows of storage tunnels is bordered on one side by an exploratory tunnel drilled into the mountain for research experiments. A cross-drift tunnel has also been drilled above the repository and through several faults.

Such intense scrutiny has resulted from the mountain's selection as a potential burial site for high-level radioactive waste. Much of this waste comes from the nation's nuclear power plants: spent fuel rods laden with highly radioactive fission products, unfissioned uranium, and plutonium. There are about a hundred commercial reactors in the United States, many operating since the sixties and seventies, and their spent fuel—some 39,000 tonnes—has been accumulating in cooling pools and dry casks with nowhere to go. By 2035, this tonnage could more than double if all power plants complete their full licensing cycles. Waste from research reactors and the Navy's nuclear fleet plus plutonium from dismantled nuclear weapons will add another 2500 tonnes. Because Congress has banned reprocessing spent fuel, all this waste must be safely stored—for eons.

A critical storage issue is the lingering radioactivity of plutonium, neptunium, and other actinides in the spent fuel. The half-lives of these elements are so long that the waste must be stored for more than 10,000 years without significant leakage to the environment. To meet Environmental Protection Agency (EPA) standards, radiation doses to the public that result from leakage must remain below 20 millirems per year (mrem/yr). These are daunting requirements for a geologic repository (see Figure 1). No matter how clever we are in engineering containment barriers—designing storage canisters and tunnels to isolate the waste—eventually, water will seep through the repository, corrode the canisters, dissolve waste radionuclides, and carry them off. When that happens, nature itself—the natural geologic barriers—will have to lend a hand in containing the waste. Studying and modeling the effectiveness of nature's barriers have been the focus of work at Los Alamos National Laboratory since the early 1980s.

In our studies, we have sought answers to a number of questions: Which radionuclides are most apt to dissolve and be carried off? How fast will they move through the rock? What radiation doses might citizens living in Amargosa Valley, the nearest community, receive if radionuclides reach the groundwater that feeds their wells? Will these doses stay below 20 mrem/yr, less than 10 percent of normal background radiation, for the next 10,000 years or more?

Reliable answers require amassing scientific data about the site's geochemistry and hydrology—for example, its groundwater chemistry, the sorption characteristics of site minerals, and potential groundwater flow paths—as well as about the radionuclides themselves. These data must then be combined to assess the performance of a complex physicochemical system over many millennia. Because no experiment can come close to analyzing radionuclide migration for 10,000 years or more, we have developed computer models to simulate the migration. These simulations are now being checked against data from extensive field tests.

Early in our work, we determined that neptunium was a leading "worst-case" radionuclide in terms of both the likelihood and consequences of its migration. As a result, much of our work has gone into characterizing neptunium's speciation, solubility, and sorption and modeling its transport. For the latter, we have developed a detailed picture of how water percolates through the mountain—in particular, what fraction will flow through fractures and what fraction will diffuse into the rock matrix. More recently, we identified colloidal transport as another pathway that must be incorporated in our modeling.

So far, our simulations show that it will take much longer than 10,000 years for neptunium to escape from the repository. In fact, it will take at least 100,000 years before there is any chance that radiation doses from escaping radionuclides could reach the EPA's limit of 20 mrem/yr. And we feel that these predictions are conservative. Key uncertainties in our transport parameters have been evaluated through sensitivity analyses, and our simulations have assumed worst-case scenarios for radionuclide release and transport.

Given the challenge of predicting complex geochemical processes on geologic time scales, however, it's not surprising that scientific debate over the repository's viability is intense. There are still many uncertainties associated with our predictions, and we are just beginning to get transport data from field experiments near Yucca Mountain that will help us validate those predictions. We are also weighing other factors, such as the likelihood of climate changes that could increase rainfall in the area and the mountain's vulnerability to volcanic activity (see the box on page 492). What follows, therefore, is a summary of work in progress at Los Alamos—of how we are developing and using computer simulations to look 10,000 years into the future, and far beyond.

Yucca Mountain Repository

To date, the Department of Energy (DOE) has spent $6 billion studying the feasibility of storing spent fuel deep within Yucca Mountain. The project involves scientists and engineers from the U.S. Geological Survey, several national laboratories, and a slew of private companies and government agencies. The task is to design a repository, characterize its site geology, and predict its reliability. By 2001, the Secretary of Energy must decide whether to recommend to the President that a repository be developed at Yucca Mountain. If the site is recommended, and if the President and Congress concur with that recommendation, then DOE will apply to the Nuclear Regulatory Commission (NRC) for a license to build the repository. As part of that application, DOE will have to present a credible case that the repository will perform as predicted.

As currently envisioned, the repository is a labyrinth of tunnels some 300 meters beneath the mountain's surface (Figures 1 and 2). Waste would be placed in steel canisters 2 meters in

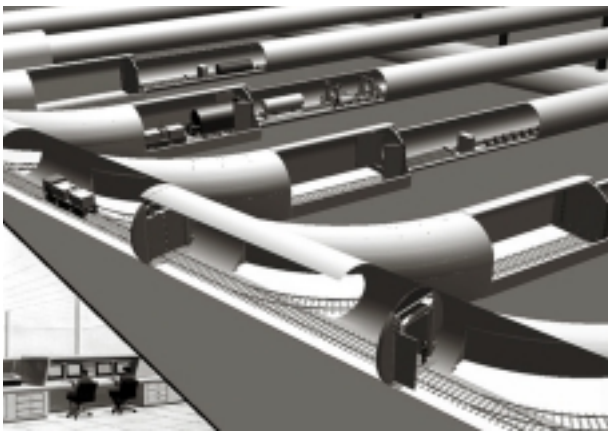

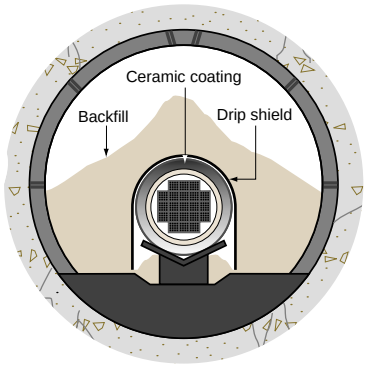

(b) Multiple Containment Barriers. The original repository design included the tunnel, floor, and support cradle. Modifications now call for enhancing containment by adding an outer ceramic coating to the waste canisters, placing an umbrella-like drip shield over them, and backfilling the tunnels.

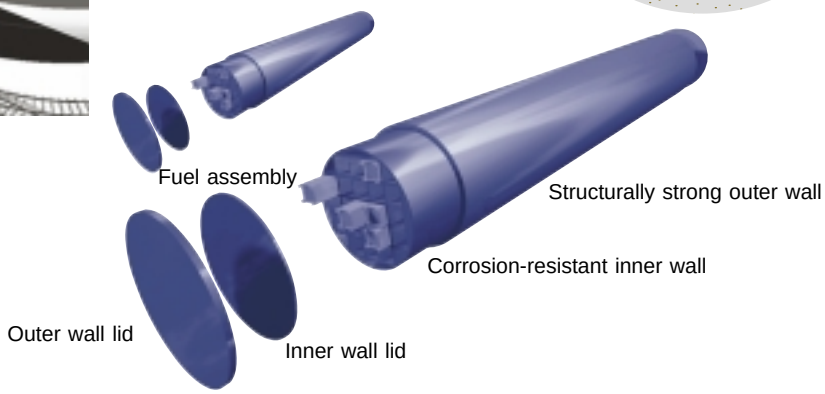

(c) Waste Canisters. Nuclear waste would be stored in double-walled, cylindrical canisters 2 m in diameter and up to 6 meters long. The initial design called for the canisters' inner wall to be made of a corrosion-resistant, high-nickel alloy almost 2 cm thick. For structural strength, the outer wall was to be carbon steel almost 10 cm thick. Recent modifications reverse the two layers.

Figure 2. Engineered Barriers at Yucca Mountain

(a) Underground Storage Tunnels. As currently envisioned, the repository consists of about 160 km of underground tunnels with access ramps and ventilation shafts. The steel- and concrete-reinforced storage tunnels and the waste canisters they would house constitute the main engineered barriers for waste isolation. After being brought in by rail, canisters would be placed on support cradles by remotely controlled cranes.

diameter and up to 6 meters long, with the canisters nestled end to end along reinforced storage tunnels. Once the repository is filled with waste (at least 70,000 tonnes), remote sensors would monitor the canisters, tunnels, and surrounding rock to make sure they function as predicted. During the first 100 years, waste could be retrieved should problems arise. Eventually, all shafts, access ramps, and tunnels would be sealed.

Two key reasons for studying Yucca Mountain as a burial site for nuclear waste are its dry climate and deep water table. The first minimizes water that could seep through the repository, corroding waste canisters and carrying off radionuclides. The mountain averages only 15 centimeters of rain a year. Of this, about 95 percent evaporates quickly, and most of the rest is taken up by plants and lost via transpiration. Only 1 or 2 percent actually soaks into the ground and percolates downward.

The mountain's low water table enables building a repository that is deep underground (300 meters) yet still in the unsaturated zone, well above the water table (another 240 to 300 meters lower). For waste radionuclides to pose a danger to the public, they will have to reach the water table and, through it, infiltrate the wells supplying water to Amargosa Valley. Several hundred meters of unsaturated rock beneath the repository pose a formidable barrier to this pathway. In addition, groundwater in the region is trapped in a closed desert basin and does not flow into any rivers that reach the ocean.

Still, rock at the depth of the potential repository contains some water. When nuclear waste is first stored in the mountain, heat from its fission products will dry out the rock, pushing moisture away from the tunnels. After about a thousand years, however, the short-lived fission products will have decayed, the temperature will drop, and water will rewet the surrounding rock. If some of the canisters have failed by then—if they have pinholes from manufacturing defects such as weak welds—dripping water could penetrate them and start dissolving radionuclides. There are many unknowns about the behavior of manmade materials subjected to heat and radiation for so long; the failure rate could accelerate, releasing more and more radionuclides into the surrounding rock.

The presence of minerals that could sop up the radionuclides is a third reason for studying Yucca Mountain as a storage site. The mountain comprises layers of volcanic tuff that were deposited millions of years ago. Many of these tuffs contain zeolites, hydrous aluminosilicate minerals that have a cagelike structure.

Zeolites are commonly used to soften hard water. Calcium and magnesium ions in water flowing through the zeolites exchange with sodium ions in the

zeolite structure and remain trapped: hard water flows in, softened water flows out. The zeolites could similarly trap radionuclides that have dissolved in groundwater. Some of the mountain's layers of zeolitic tuff also contain clay, another sorbing material. The zeolites and clay could effectively remove strontium and cesium and, to a lesser but still significant extent, uranium, plutonium, neptunium, and other transuranics that have leached into groundwater seeping through the repository and toward the water table.

Modeling the Mountain

Work at Los Alamos in developing a radionuclide transport model for Yucca Mountain began by incorporating the mountain's stratigraphy into computational grids. Using techniques that ranged from x-ray diffraction and fluorescence to microautoradiography and potassium/argon dating, we analyzed hundreds of borehole samples taken from the mountain. The picture that emerged from these and other analyses is that the mountain is composed of alternating layers of welded and nonwelded tuff—volcanic ash—that are tilted, fractured, faulted, and locally altered to zeolites and clay minerals (Figure 3).

The welded tuff consists of dense, nonporous deposits that have been hardened by heat and pressure and are typically highly fractured. By contrast, the nonwelded tuffs are soft, porous deposits that contain few fractures. Three significant zeolitic layers underlie the repository site: one in the unsaturated zone, one in the saturated zone, and one that slopes downward through both zones. A thin layer containing clay and zeolites also stretches beneath the repository.

One important finding from our rock analyses is that zeolites and clays pose effective natural barriers to radionuclide migration. Sorptive zeolites (clinoptilolite and mordenite) offer the most massive and mappable barrier. Whether their interactions are strong, as with strontium and cesium, or weak, as with neptunium, their sheer abundance makes them a formidable obstacle to radionuclide transport. Smectite clays are not so abundant, but their widespread occurrence ensures that all transport pathways will eventually encounter them. The clays' strong affinity for plutonium and moderate affinity for neptunium make them an effective barrier. One other mineral group, manganese oxides, should also function as a barrier. Although these oxides are not so abundant or widely distributed as the clays (and consequently not "mappable"), they commonly coat fracture surfaces in both the saturated and unsaturated zones. Their strong interaction with neptunium should impede the latter's transport through fractures.

Our transport model incorporates these various stratigraphic layers, including their mineral compositions, porosities, fault locations, and fracture densities. It also incorporates hydrological data from the U.S. Geological

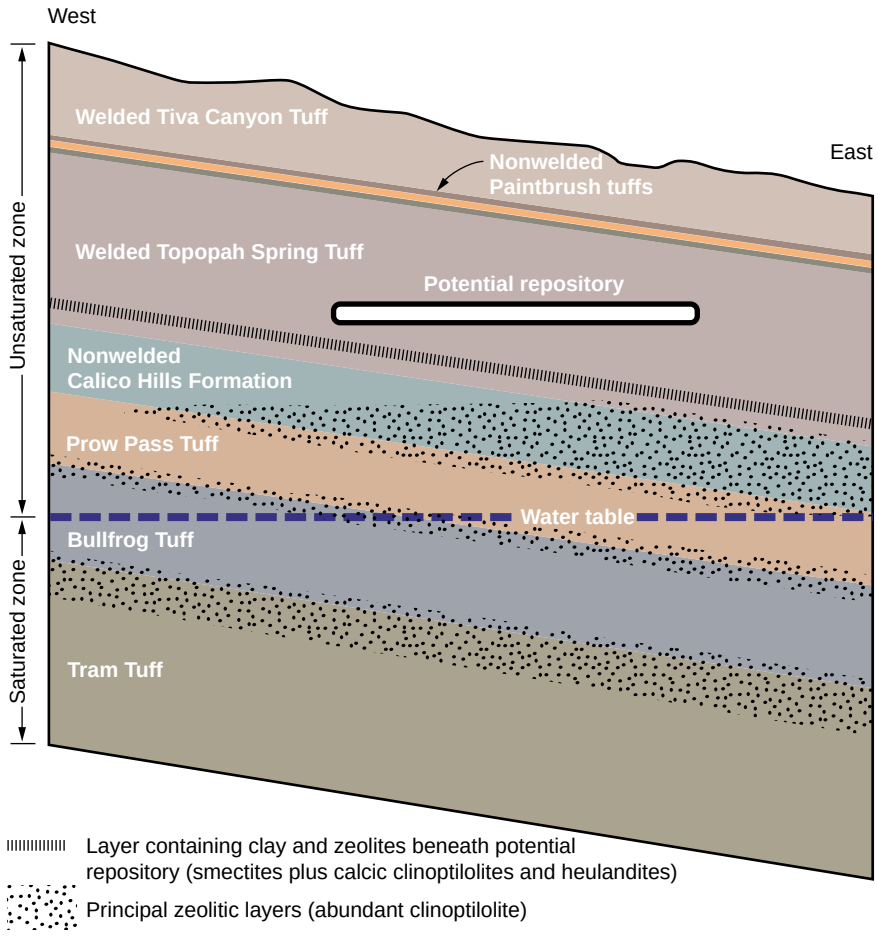

Figure 3. Yucca Mountain Stratigraphy

This east-west cross section of Yucca Mountain shows the potential repository relative to the water table and principal rock strata. The main upper layers of volcanic ash alternate between welded tuff (highly fractured, dense volcanic deposits) and nonwelded tuff (highly porous deposits with few fractures). The clay-altered layer of nonwelded Paintbrush tuffs above the repository is expected to impede the percolation of water from the mountain's surface toward the repository. The zeolitic layers beneath the repository could filter out or slow down radionuclides that escape the repository's engineered containment barriers and move toward the saturated zone. (Note: the vertical scale in this cross section is exaggerated.)

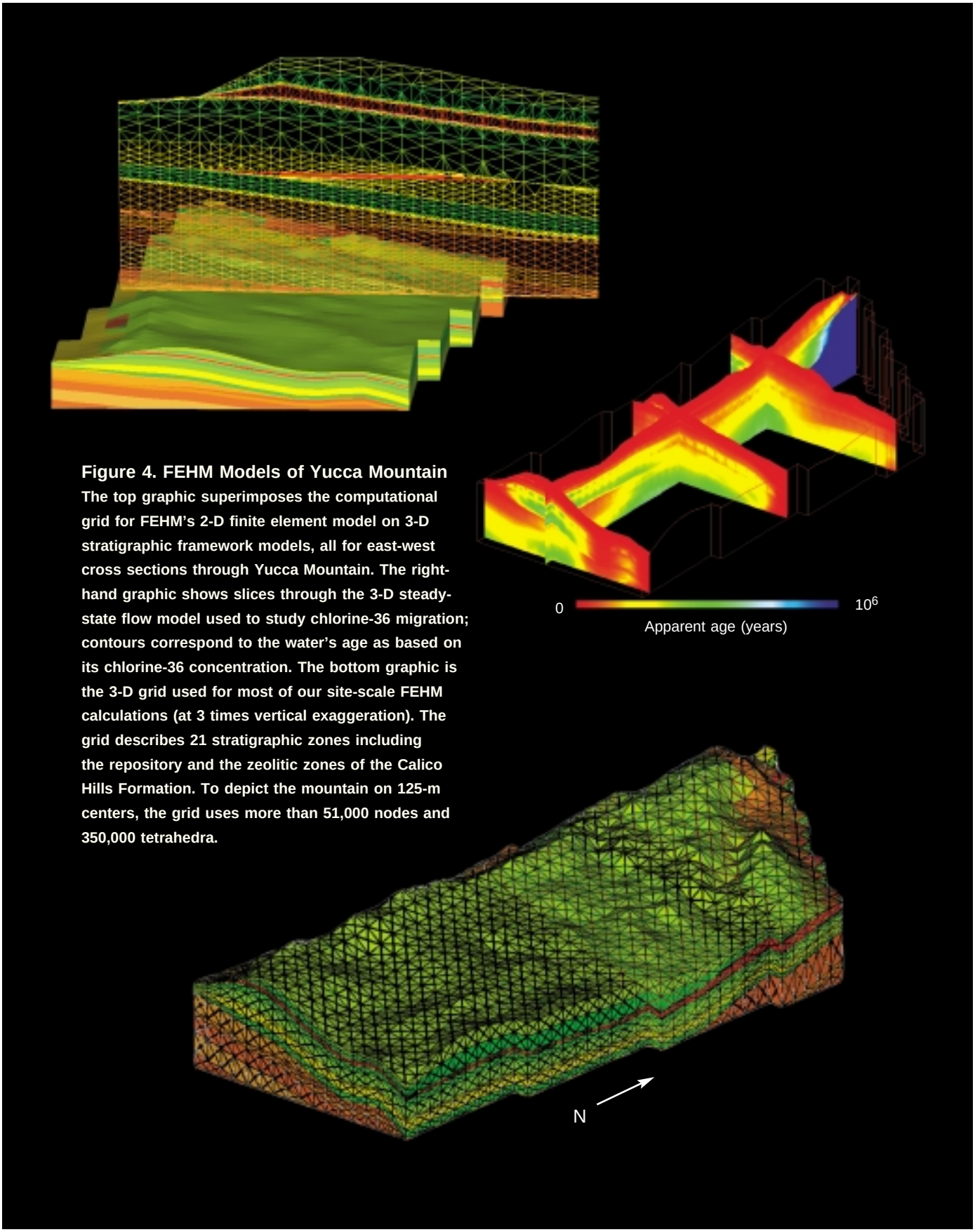

Figure 4. FEHM Models of Yucca Mountain
The top graphic superimposes the computational grid for FEHM's 2-D finite element model on 3-D stratigraphic framework models, all for east-west cross sections through Yucca Mountain. The right-hand graphic shows slices through the 3-D steady-state flow model used to study chlorine-36 migration; contours correspond to the water's age as based on its chlorine-36 concentration. The bottom graphic is the 3-D grid used for most of our site-scale FEHM calculations (at 3 times vertical exaggeration). The grid describes 21 stratigraphic zones including the repository and the zeolitic zones of the Calico Hills Formation. To depict the mountain on 125-m centers, the grid uses more than 51,000 nodes and 350,000 tetrahedra.

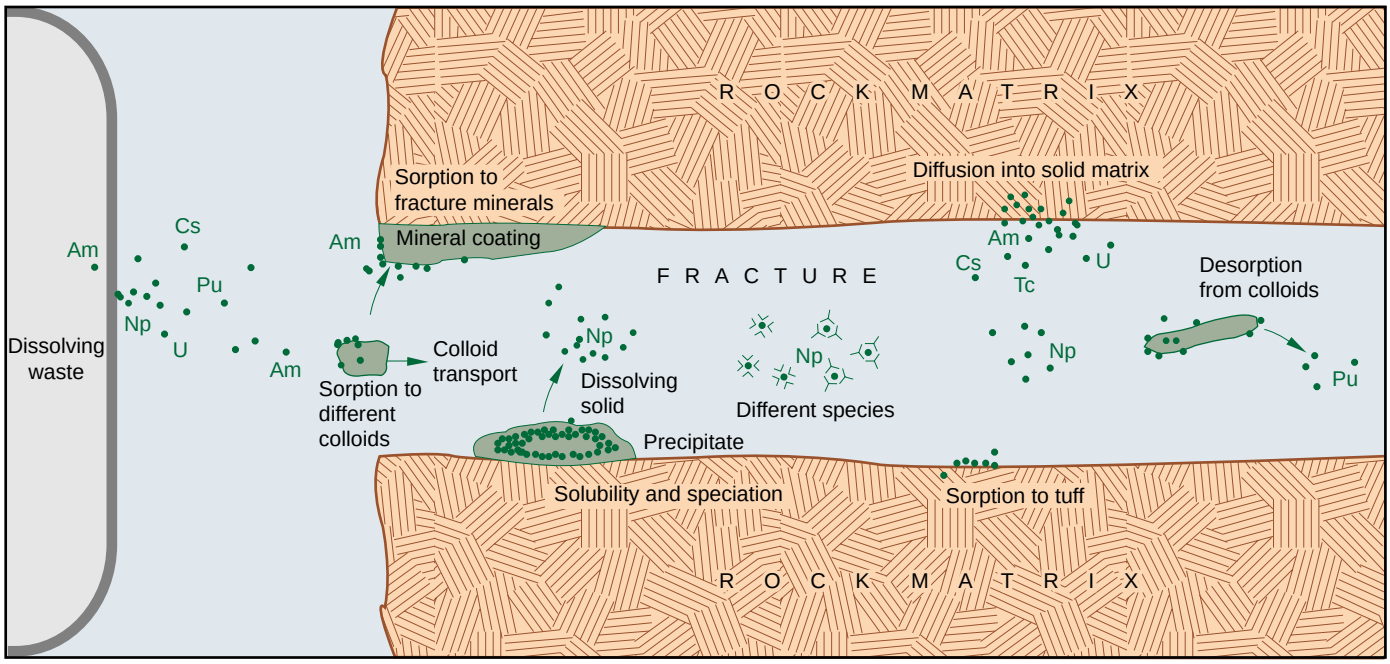

Figure 5. Geochemical Factors for Radionuclide Transport

This cartoonlike depiction of a breached waste canister shows how dissolved radionuclides could escape from the repository through water-filled rock fractures and how the surrounding rock matrix could impede their escape. To assess the effectiveness of Yucca Mountain's geologic barriers in slowing radionuclide transport, we have conducted laboratory-scale experiments to learn how soluble the radionuclides, particularly neptunium-237, would be in mountain groundwater, to what extent they would be removed from the water by sorption onto mountain tuffs and fracture minerals or by diffusion into the rock matrix, and how colloids (nanometer-sized particles) would affect their transport through rock fractures. Data from these studies are important in defining the chemical and physical parameters for our modeling.

Survey and from Lawrence Berkeley National Laboratory. These data include rock matrix and fracture permeability, residual water content in the tuff, and a spatial map of precipitation infiltration along the mountain's surface. Finally, the model incorporates radionuclide transport properties derived from extensive laboratory experiments, such as radionuclide solubilities in Yucca Mountain groundwater, sorption coefficients for the various tuffs, and diffusion coefficients for the movement of dissolved radionuclides in the rock matrix.

The nexus for all these data is FEHM—a finite element heat- and mass-transport code. FEHM solves the equations of heat and mass transport in porous and fractured media in two or three dimensions. The code also offers a comprehensive set of models for simulating the transport of dissolved species in either the gas or liquid phase. It combines the capability of simulating transport using either finite element or particle-tracking solutions with a dual-permeability capability that captures the effect of fractures on flow and transport.

The code is linked to software that produces finite element computional grids that not only preserve the site's hydrostratigraphic structure but also honor the numerical conditions needed to perform accurate simulations. The grids, or meshes, are made of triangles for 2-D models and tetrahedra for 3-D models (Figure 4). Using the physical and chemical properties we have tied to each node in the calculation grids, FEHM calculates, in discrete spatial and temporal steps, the transport of individual radionuclides through the mountain. (See the box on the following two pages for an explanation of mesh generation.)

Figure 5 shows the geochemical factors for radionuclide transport that we have focused on in assessing the effectiveness of Yucca Mountain's geologic barriers. Percolating groundwater is the primary carrier for the radionuclides, which are all soluble in water to some extent. After dissolving, they must travel through the repository's backfill and heat-altered tunnel walls, through the unsaturated rock beneath the repository, and finally through the saturated zone's groundwater flow system. In addition to the hydrologic processes that are important to radionuclide migration, transport processes such as sorption onto minerals and diffusion into dead-end rock pores will control the ultimate movement of radionuclides. Findings at the Nevada Test Site of colloid-facilitated transport for actinides have added yet another process of concern, which is discussed in the box on page 490). To be credible, our transport models must account for all these processes.

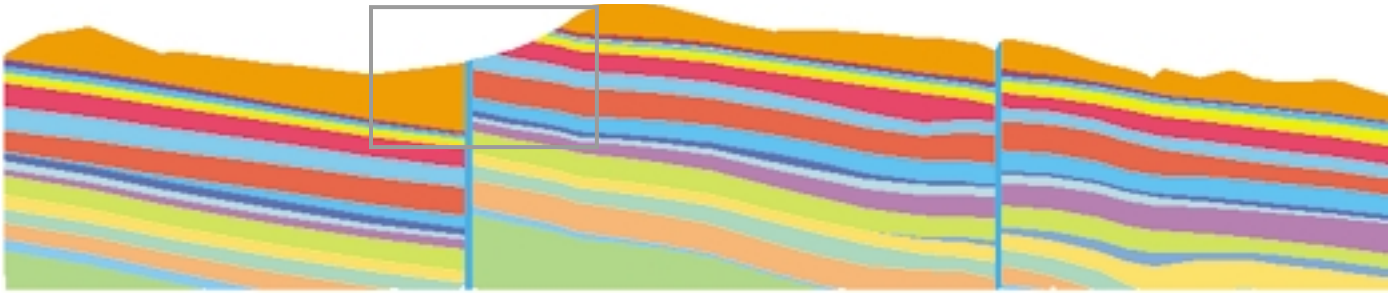

(a) Geological Model of a Cross Section at Yucca Mountain

Mesh Generation for Yucca Mountain

Carl W. Gable

To model the transport of waste radionuclides through Yucca Mountain, we must generate a grid, or mesh, on which our FEHM calculations can be run. Our primary tool for generating, optimizing, and maintaining computational meshes is LaGriT (for Los Alamos Grid Toolbox), a general-purpose software package. LaGriT is a spinoff of X3D, which was developed in the 1980s by Harold Trease.

Developed in the 1990s, LaGriT is a collaborative product of the Applied Physics, Theoretical, Earth and Environmental Science, and Computing, Information, and Communications Divisions at Los Alamos. It has been used to model such varied phenomena as shock physics, combustion, semiconductor devices and processes, biomechanics, the evolution of metallic microstructure, porous flow, and seismology.[1]

A mesh consists of nodes (points) at specific locations in space that are connected to form elements. These elements can be triangles or quadrilaterals in 2-D models and tetrahedra, hexahedra, prisms, or pyramids in 3-D models. The elements fit together like the pieces of a puzzle to represent physical systems such as the rock layers in Yucca Mountain, a human knee joint, or a semiconductor chip. Physical quantities such as pressure, temperature, or density, which are continuous in real materials, are usually represented by discrete values at the nodes or within the elements.

Mesh generation draws on both creativity and advanced mathematical algorithms. As Thompson et al. (1999) note, grid generation is "still something of an art, as well as a science. Mathematics provides the essential foundation for moving the grid generation process from a user-intensive craft to an automated system. But there is both art and science in the design of the mathematics for . . . grid generation systems, since there are no inherent laws (equations) of grid generation to be discovered. The grid generation process is not unique; rather it must be designed."[2]

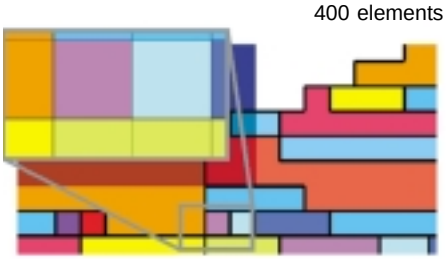

(b) Low-Resolution Regular Mesh

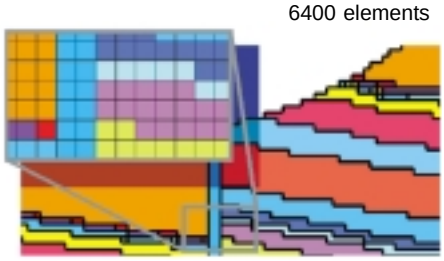

(c) High-Resolution Regular Mesh

Mesh generation can be automated but never becomes automatic. Although software like LaGriT helps automate complex "meshing" operations, generating successful meshes still rests on a series of judgment calls by an expert, who must weigh many tradeoffs. For example, imagine a calculation done on a $10 \times 10 \times 10$ grid of hexahedral elements. If we double the resolution to a $20 \times 20 \times 20$ grid, the total number of elements goes from 1000 to 8000. In addition, if the calculation involves modeling the change over time of a quantity such as saturation, doubling the resolution may require cutting the time steps in half, which doubles the computer time needed. Overall, then, doubling the calculation's resolution will increase calculation time by a factor of 16. Although high resolution best represents complex geometry and produces the most accurate physics solution, it requires more elements, which result in calculations that require more computer memory and cycles.

The accompanying graphics illustrate various computational grids that could be generated for modeling Yucca Mountain. Our starting point is a geological model that represents the mountain as a sequence of sloping rock layers offset by two vertical faults (a). Focusing on the boxed area around the left-hand fault, we first create a simple mesh of square elements (b). The elements' colors correspond to those of the cross-section layers they represent

[1]More information on LaGriT is available from the software's Web site: http://www.t12.lanl.gov/~lagrit/.

[2]*Handbook of Grid Generation*. 1999. J. F. Thompson, B. K. Soni, and N. P. Weatherill, Eds. New York: CRC Press, p. iii.

and thus also to the layers' varying material properties (such as density and porosity).

The low-resolution squares in (b) do a poor job of representing the geology. The vertical fault is lost and individual rock layers are nearly lost because the mesh is so coarse. We can improve the mesh by increasing its resolution: the squares in (c) are one-quarter the size of those in (b). Now the geology is better represented, although the interfaces between rock layers are still represented by jagged stair steps. Also, only the thickest layers are represented by contiguous elements; thin layers and small features are still lost in the grid's coarseness.

Another approach is to use variable mesh spacing, as shown in (d). Variable spacing allows us to "zoom in" with high resolution on some areas and maintain low resolution in others. However, variable spacing generally works well only for simple geometries in which the phenomena being modeled take place in a small portion of the entire computational domain and thus only a few areas require high resolution.

A more flexible approach is to adapt mesh resolution to the geometry of interest, as done in the quad-tree meshes shown in (e) and (f). These meshes allow cascading refinements: each element is subdivided into four elements, each of which is then subdivided into four still smaller elements, and so on.

In (e) and (f), we start with the mesh of (b) and then refine only selected elements. In (e), we refine along all material interfaces by a factor of 16 but leave regions far from these interfaces at low resolution. In (f), we refine only thin rock layers by a factor of 32, increasing their resolution while maintaining lower resolution in the thick layers. In both cases, however, the number of elements is much greater than in the previous meshes, which will slow down our calculations.

Our mesh examples so far are all structured: that is, they are made of quadrilateral elements whose positions are readily defined in terms of rows and columns and whose connectivity is logical. Our last mesh examples are made of unstructured triangular elements whose connectivity is more arbitrary: for example, the nodes have varying numbers of triangles attached to them. This unstructured approach, however, allows us to create meshes that actually conform to the mountain's varied material interfaces.

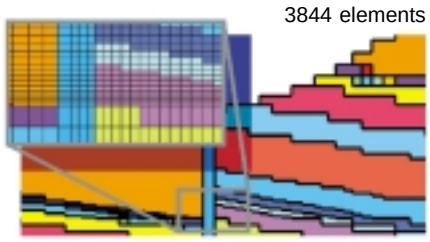

(d) Variably Spaced Regular Mesh

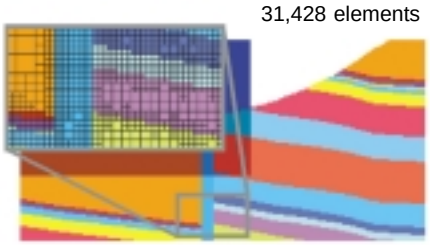

(e) Quad-Tree Mesh

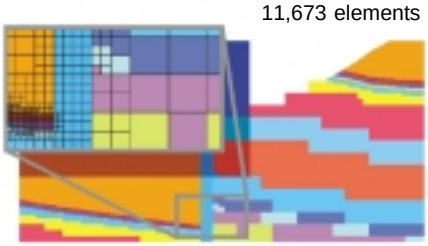

(f) Quad-Tree Mesh

Both low-resolution (g) and high-resolution (h) meshes do well in representing the geologic interfaces. The high-resolution mesh, however, will do a better job solving the physics of radionuclide transport because its smaller elements can more accurately represent variations that occur over short distances. In modeling Yucca Mountain, we must also contend with phenomena that lack symmetry, have a wide range of length scales, and involve very thin layers that must be preserved as continuous. As a result, triangles in 2-D modeling and tetrahedra in 3-D modeling have been our meshes of choice.

In addition to tradeoffs in how well they represent the mountain's geometry, meshes also pose tradeoffs in their suitability for different physics codes. Some codes can solve problems only on regular grids like those shown in (b)–(d). Others can use quad-tree meshes like those shown in (e) and (f) but not the unstructured meshes of (g) and (h). Thus the meshing approach must be compatible with the physics code that will be used.

Developing flow and transport models for Yucca Mountain has pushed the limits of mesh generation technology. The models' size requires us to keep the number of elements as low as possible, their complex physics requires us to accurately represent the geology of the repository site, and the need for timely results requires us to automate mesh generation whenever possible. These often conflicting demands have been met by a collaborative effort in enhancing mesh generation capabilities to meet the challenges of modeling Yucca Mountain. ■

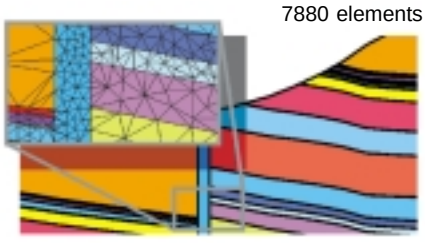

(g) Low-Resolution Triangular Mesh

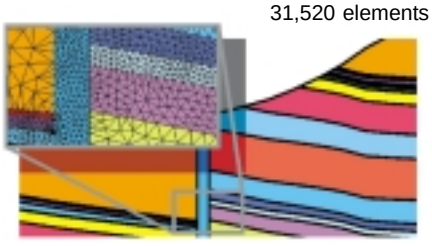

(h) High-Resolution Triangular Mesh

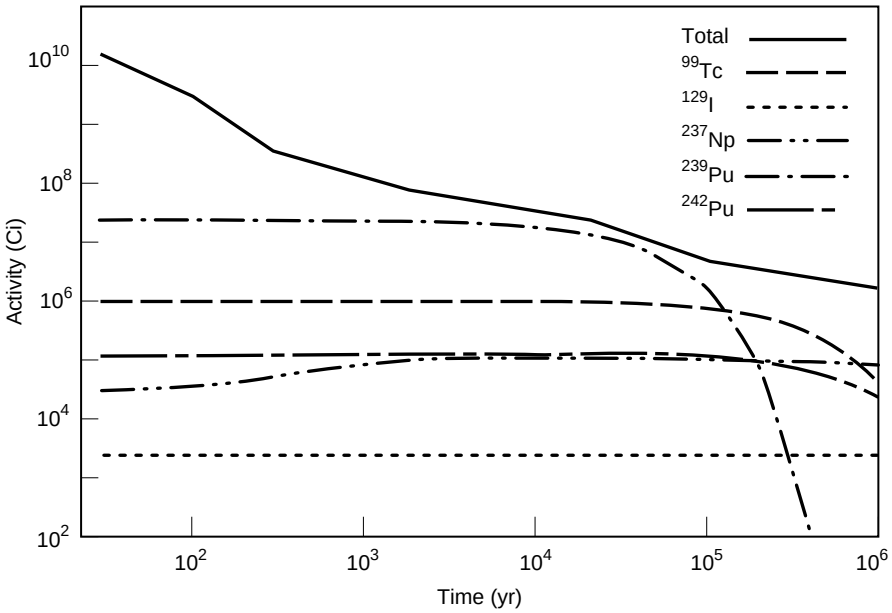

Figure 6. Radionuclide Decay Rates for Nuclear Waste

The waste's initial activity (first 1000 years) is primarily a result of short-lived fission products. Having fallen about three orders of magnitude, the remaining activity is then a result of technetium-99, iodine-129, and three long-lived actinides: neptunium-237, plutonium-239, and plutonium-242.

Neptunium Chemistry

Of the several hundred radionuclides present in spent fuel, only six are long-lived, soluble, mobile, copious, and hazardous enough to contribute significantly to calculated radiation exposures should the nuclides reach well water in Amargosa Valley. Four of them (technetium-99, iodine-129, uranium-234, and neptunium-237) could be transported by groundwater because of their high solubility and weak adsorption to minerals. The other two (plutonium-239 and plutonium-242) tend to adsorb to minerals (because of their IV oxidation state) but could be transported on or as colloids.

Although technetium-99 and iodine-129, both abundant in spent fuel, would be the dominant radionuclides to reach the valley in the first 10,000 years (Figure 6), radiation doses from them are not expected to exceed EPA limits. After 10,000 years, neptunium-237 starts to become the radionuclide of concern. While neptunium concentrations in spent fuel are small (only 0.03 percent), they will increase over time through the decay of americium-241, which has a half-life of 432.7 years. Because of its radiotoxicity, long half-life (2.14×10^6 years), high solubility, and relatively low sorption on Yucca Mountain tuffs, neptunium has been the radionuclide of prime concern in our transport calculations. Thus we have conducted extensive laboratory tests to determine its solubility, speciation, sorption, and transport. Understanding neptunium's chemical behavior is fundamental to modeling its transport.

Solubility. As in most natural aquifers, Yucca Mountain groundwater contains a number of dissolved species that can interact with the radionuclides and alter the latter's solubility. Radionuclides such as neptunium, technetium, and plutonium are also very sensitive to changes in the water's redox potential and pH. Such changes affect the stability of the radionuclides' oxidation state, which is the main parameter that controls the extent of their geochemical reactions.

Table I characterizes groundwater drawn from two saturated-zone wells and pore water found in the unsaturated zone at Yucca Mountain. Because carbonate is the predominant ligand for neptunium complexation, and because the two saturated-zone waters roughly bracket the bicarbonate concentrations found at Yucca Mountain, we have used their chemistries in our transport calculations.

Under oxidizing conditions (i.e., in water with a redox potential of >200 millivolts), neptunium will be stable in the V oxidation state, which generally has the highest solubility among actinide oxidation states. However, reducing conditions from oxygen depletion may exist in saturated-zone water at Yucca Mountain given the presence of low-valent iron. These conditions would stabilize neptunium in the IV oxidation state and reduce its solubility by several orders of magnitude. While research is still ongoing, current data strongly support the existence of some reducing groundwaters in the saturated zone at Yucca Mountain.

Carbonate concentrations, which at Yucca Mountain are in the millimolar range, will have an important effect on neptunium transport. In typical groundwaters, NpO_2^+ and the monocarbonate complex, $NpO_2CO_3^-$, are the predominant neptunium solution species. With decreasing carbonate concentration, NpO_2^+ and, to a lesser extent, the first hydrolysis product, $NpO_2OH(aq)$, will dominate the solution speciation. Changes in species composition and charge will change neptunium's sorption, which in turn will alter its transport characteristics. Speciation changes may be expected in different site-specific groundwaters and when going from unsaturated- to saturated-zone water.

Under different physicochemical conditions, neptunium can either accumulate and form a precipitate after oversaturation or be transported by groundwater as dissolved or particulate species. Over time, the precipitates formed initially may transform to more thermodynamically stable and thus less

Table I. Chemistry of Yucca Mountain Groundwater

Concentrations of the major dissolved species in water from two saturated-zone wells and in pore water from the unsaturated zone. In our calculations, we have used the two saturated-zone waters to bracket the water chemistries expected at the potential repository.

	Saturated-Zone Well Water (mg/L)		Unsaturated-Zone Pore Water (mg/L)
Species			
Sodium	45	171	26–70
Bicarbonate	143	698	20–400
Calcium	12	89	27–127
Potassium	5	13	5–16
Magnesium	2	32	5–21
Sulfate	18	129	39–174
Nitrate	10	<0.1	0–40
Chloride	6	37	34–106
Fluoride	2	4	–
Silicon	30	30	72–100
pH	6.9	6.7	6.5–7.5
Eh (mV)[a]	340	360	400–600[b]

[a]Redox potential
[b]May be lower locally

soluble solid phases. Despite the importance of carbonate for neptunium speciation in solution, however, solid Np(V) carbonates with the general formula $MNpO_2CO_3 \cdot nH_2O$, where M is any alkali, are not likely to be stable because of the low concentrations of alkali metal cations in Yucca Mountain groundwaters. Thus, solid Np(V) oxides and/or hydroxides determine neptunium's solubility in mountain groundwaters. At redox potentials lower than about 300 millivolts, Np(IV) oxide/hydroxide is the solubility-controlling neptunium solid, with Np(V) predominating in solution.

In transport and dose calculations, our current solubility limit for neptunium is about 10^{-4} molar, with minimum and maximum values of about 10^{-6} and 10^{-3} molar, respectively. By comparison, the solubility limit for plutonium is around 10^{-8} to 10^{-7} molar, three orders of magnitude lower than that of neptunium. Plutonium's lower solubility results from the existence of Pu(IV) in the solid state. Neptunium's much greater solubility drives the search to find reducing conditions as an additional barrier to neptunium transport at Yucca Mountain.

Sorption. Once groundwater dissolves the radionuclides and begins to carry them away from the repository, their sorption on mineral surfaces is the main geochemical mechanism for limiting their migration. As described earlier, Yucca Mountain is composed of a thick (>1.5 kilometers) layered sequence of volcanic tuffs and lavas (see Figure 3).

To determine the mineral composition of these layers, we analyzed thousands of core samples from the many wells that penetrate the mountain and surrounding area. These analyses show that the tuffs can be classified as vitric, devitrified, and zeolitic. Vitric tuff is composed primarily of volcanic glass fragments. Devitrified tuff, present in more than half the layers, is composed of glass fragments that have crystallized into an assemblage of feldspars and silica minerals, forming densely welded stratigraphic units. Zeolitic tuff is composed mostly of volcanic glass that has been altered to zeolites.

To characterize the transport behavior of radionuclides within these layers, we measured radionuclide sorption onto the tuffs and, for comparison, onto pure, well-characterized minerals. Crushed tuff and mineral samples were equilibrated with groundwater typical of Yucca Mountain before the radionuclides were added. From the measured amounts of radionuclides remaining in solution (C) and sorbed onto the substrate (F), we then calculated the batch sorption coefficient, $K_d = F/C$.

The K_d value (in milliliters per gram) is the ratio of moles of radionuclide per gram of solid phase to moles of radionuclide per milliliter of solution. A large K_d value indicates high sorption on the mineral or tuff.

Table II gives values for neptunium and plutonium sorption onto samples of vitric, devitrified, and zeolitic tuff and onto several minerals. As expected, the highest sorption coefficients for neptunium are obtained for zeolitic tuff and clay-bearing vitric tuff. The same sorption behavior would be expected for neptunium and plutonium ions in the same oxidation state. The fact that plutonium has a much higher retention via sorption than neptunium most likely reflects the nuclides' presence in different oxidation states: Np(V) and Pu(IV). The low sorption of neptunium is due to the small charge-to-radius ratio, the large size, and the low tendency for complexation reactions of the neptunyl ion (NpO_2^+). Because of steric effects, the sorption mechanism for neptunium onto a zeolite may be a surface reaction rather than cation exchange within the zeolite's cagelike structure.

We found that neptunium sorption for multiple tuff samples is actually rather variable. Some zeolitic, vitric, and devitrified tuff samples have almost no affinity for neptunium, whereas other samples with similar mineral compositions show sorption coefficients in the range of 5 to 10 milliliters per gram (mL/g). This variation suggests that the favorable sites for sorption are associated with some minor mineral phases, such as iron oxides or clays,

whose abundance varies in the tuff. Indeed, the largest values for neptunium sorption in Table II are for the pure minerals hematite (an iron oxide) and calcite (calcium carbonate) and for smectite (a clay). Experiments with pure clinoptilolite, a common zeolite in Yucca Mountain tuffs, and tuff samples containing significant amounts of clinoptilolite show that neptunium sorption increases with decreasing pH, contrary to the sorption of other radionuclides onto zeolites. Given the relative abundance of clinoptilolite at Yucca Mountain, we have found that a reasonable approach for predicting the sorption of neptunium onto zeolitic tuffs is to assume that clinoptilolite is the only sorptive mineral present.

Because one of the main components of Yucca Mountain groundwater is bicarbonate, we also examined how neptunium sorption is influenced by the groundwater's carbonate content and ionic strength. Although calcite showed an increase in neptunium sorption as carbonate content and ionic strength increased, zeolitic tuff showed a decrease in sorption. Such behavior is indicative of different sorption mechanisms for the two substrates.

Sorption Mechanisms. If we assume that clinoptilolite is the only sorbing phase for zeolites and calculate values of K_d divided by the solid-phase surface area, we find that neptunium sorption onto a series of tuff samples is correlated with surface area (Figure 7). This correlation again suggests that sorption is a surface reaction rather than cation exchange throughout the volume of the zeolite. Based on such data, we feel that neptunium sorption onto Yucca Mountain minerals is governed by surface complexation on a variety of oxide phases and by coprecipitation and surface adsorption involving carbonate minerals, such as calcite.

The surface-complexation mechanism appears to be relatively insensitive to variations in ionic strength, groundwater composition, and pH values between 6.5 and 8.5.

Table II. Comparison of Sorption Coefficients for Neptunium and Plutonium

	K_d (mL/g)[a]		
	Neptunium		Plutonium
Samples	pH = 7	pH = 8.5	pH = 7
Tuffs			
Zeolitic tuff	0.30	1.5	300–500
Devitrified tuff	0.007	–0.04	40–100
Vitric tuff	0.2	0.3	600–2,000
Vitric tuff with 10% clay	–8	—	—
Minerals			
Quartz	–0.1	–0.2	<10
Albite	–0.08	–0.1	3–10
Calcite	—	50	200–1,000
Hematite	70	600	>10,000
Clay			
Smectite	80	—	—
Zeolite			
Clinoptilolite	2.6	1.4	600–3,000

[a]Negative values are due to uncertainties in the data (±0.5).

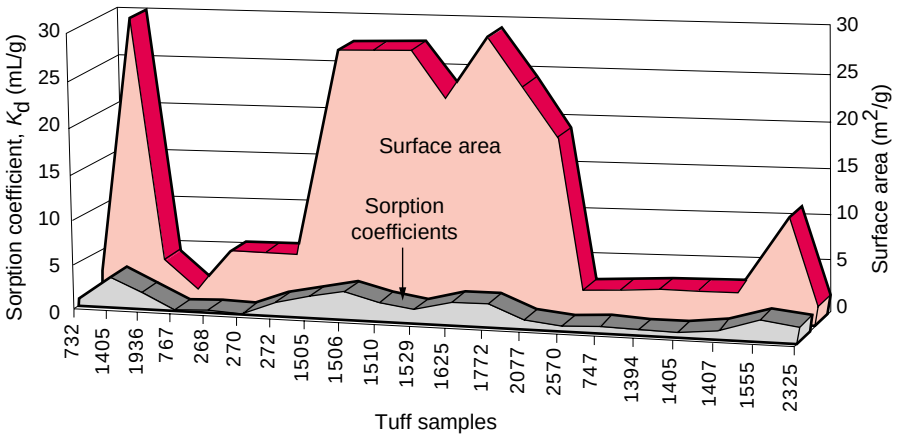

Figure 7. Correlation of Neptunium Sorption and Tuff Surface Area
Comparison of the coefficients for neptunium sorption onto various tuff samples and the samples' surface area shows the two values to be correlated. The sorption coefficients are for neptunium solutions in typical Yucca Mountain groundwater under atmospheric conditions and at initial neptunium concentrations of about 10^{-7} M.

This mechanism is likely responsible for the 0.5- to 5.0-mL/g range in neptunium sorption coefficients measured in many different rock samples. The high end of this range may reflect secondary mechanisms, such as the reduction of Np(V) to Np(IV) on mineral surfaces containing ferrous iron, making the actinide more strongly sorbing. Because of these uncertainties concerning sorption mechanisms, we have used a probability distribution for neptunium sorption coefficients in our transport calculations for Yucca Mountain.

Dynamic Measurements. In contrast to the batch sorption equilibrium measurements discussed above, the migration of radionuclides through tuff is a dynamic, nonequilibrium process. Thus, we needed to confirm our equilibrium measurements by carrying out dynamic transport experiments. We did this by eluting radionuclide solutions through columns of washed, crushed, and saturated Yucca Mountain tuff, using the same tuff as in our batch sorption experiments. (Migration through a solid rock column under unsaturated conditions would require more time than was feasible for our work.)

The arrival time for neptunium at the bottom of the column was consistent with the sorption coefficients measured in our batch sorption experiments. Consequently, we can predict the retardation of neptunium transport simply by using the equilibrium sorption coefficient. However, while the elution time was accurately predicted, the amount of eluted radionuclide differed from modeling predictions. The radionuclide did not travel uniformly through the column but arrived dispersed, probably because of variable path lengths through the rock.

A key implication of these dynamic measurements is that the use of batch sorption values in site calculations will yield conservative predictions. In other words, the predicted radionuclide transport times to the repository's site boundary (defined as 5 kilometers distant) will be shorter than actual travel times. Thus, if the simulations show that the natural rock barriers effectively impede neptunium transport, then uncertainties associated with neptunium sorption mechanisms will only improve the barriers' effectiveness over our predictions for them.

Matrix vs Fracture Flow

Another key issue for radionuclide transport is groundwater flow—how quickly will water move through the mountain and what pathways will it follow? Early theories ranged from a "tin roof" scenario in which the upper thin layer of nonwelded tuffs acts as a relatively impervious barrier, diverting water laterally and drastically reducing percolation through the repository, to a scenario of rapid flow along major faults and fractures that allows water to infiltrate the repository within only a few decades. Our studies have shown the actual flow mechanisms to be a bit more complex than either of these two extremes.

To assess the movement of groundwater through Yucca Mountain, we began by looking at how water enters its upper surface. Scientists from the U.S. Geological Survey have measured infiltration rates, conducting neutron assays of soil moisture to a depth of 75 meters. By balancing such parameters as precipitation, runoff, evaporation, soil thickness, plant transpiration, and hydraulic rock properties, they developed a spatial map of infiltration across the surface of the mountain. According to this map, infiltration is highest along the crest, where rain clouds accumulate and soil cover is almost nonexistent, and much lower where thick alluvial deposits and relatively abundant plant life lead to high rates of evapotranspiration.

Next, we augmented the survey data by examining the water content in rock samples taken from deeper within the mountain. As wells were bored, we analyzed pore water trapped in core samples at various depths to determine its age and infiltration rate. Also, when an exploratory tunnel was drilled into the mountain, we collected hundreds of rock samples at regular intervals along its length. This 8-kilometer-long, U-shaped tunnel descends to the level of the potential repository and parallels the repository's eastern boundary along its own curved base (see Figure 1). The tunnel intersects major fractures in the mountain that are due to faulting, tilting, and block rotation in the distant past.

We analyzed the pore water in these rock samples for its chlorine concentration. Because chloride salts are highly soluble, they dissolve in rainwater and move into the mountain with the infiltrating water. Once water has traveled through the upper soil zone, where it can evaporate or be taken up by plants, its chloride concentration remains relatively constant. Comparing the chloride concentration in pore water below this zone with that in rainwater yields a measure of how much water has been lost to evaporation and, thus, allows us to determine net infiltration rates for the mountain.

In addition, chlorine has a radioactive isotope, chlorine-36, that is produced naturally in the atmosphere by the interaction of cosmic rays with argon. Because the amount of chlorine-36 so generated has changed over the ages and because the isotope's half-life is 300,000 years, the ratio of chlorine-36 to stable chlorine (^{36}Cl/Cl) in groundwater serves as a measure of the water's age.

Looking back tens of thousands of years, we find that the ^{36}Cl/Cl ratio has varied because of variations in chloride deposition rates (perhaps due to climate changes) and variations in chlorine-36 production (due to changes in the earth's geomagnetic shielding). A broad-brush picture shows a bimodal distribution: a fairly constant ^{36}Cl/Cl ratio of about 5×10^{-13} over the last 10,000 years (the Holocene signal) and an elevated ratio of about 10×10^{-13} before that period (the Pleistocene signal). We confirmed this bimodal distribution by analyzing fossilized pack-rat middens (replete with crystallized urine) for chlorine-36 and plotting the measurements against their radiocarbon ages.

During the 1950s and early 1960s, a chlorine-36 spike occurred when atmospheric nuclear tests in the South Pacific significantly increased the isotope's production rate. The resulting ^{36}Cl/Cl ratio rose above 15×10^{-13}. This "bomb pulse" can be used to test for recent groundwater, such as would be expected if water infiltrated Yucca Mountain by way of fast transport paths through fractures and faults.

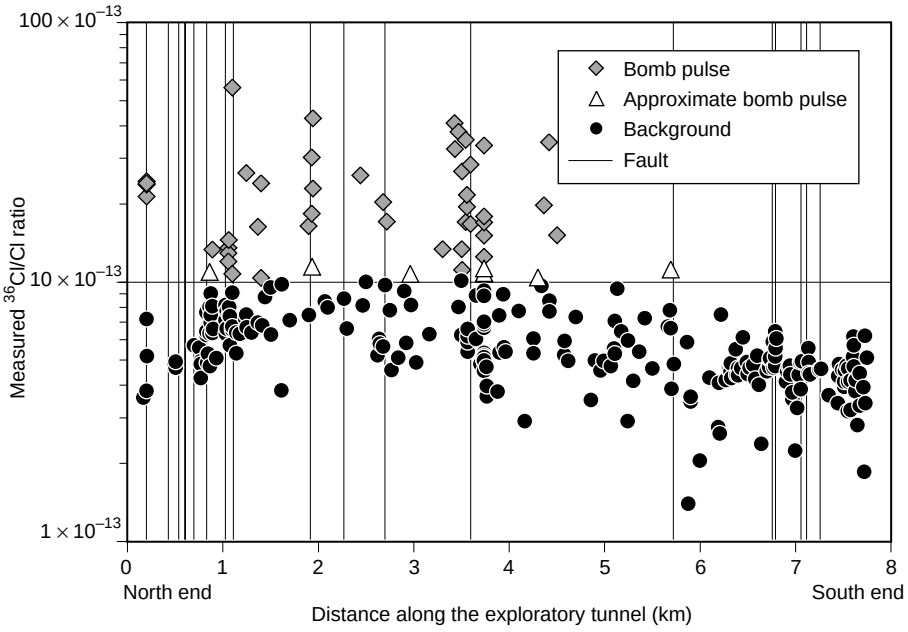

Figure 8. Distribution of ^{36}Cl/Cl Ratios in Pore Water from Exploratory Tunnel Rock Samples

Most bomb-pulse water is associated with faults (vertical lines). At the southern end of the tunnel, however, no bomb-pulse water was found even though faults are present. At both ends of the tunnel, but especially at the south end, the ^{36}Cl/Cl ratio drops off, indicating that these regions contain predominately Holocene water (<10,000 years old). By contrast, the north-central part of the tunnel has predominately Pleistocene water (>10,000 years old). These variations likely result from the changing thickness of the Paintbrush tuffs above the tunnel: where they are thicker, the travel time for water is longer.

When the pore-water data from the tunnel rock samples were examined statistically, we found four distinct sets of ^{36}Cl/Cl ratios. The two main ratios were the expected Holocene and Pleistocene signals. A small set of lower ratios in which chlorine-36 had noticeably decayed may represent water that is 300,000 years or more old. Finally, a small set of elevated ^{36}Cl/Cl ratios (12×10^{-13} and greater) represents very young bomb-pulse water.

We found a strong correlation between the distribution of bomb-pulse water and major faults (Figure 8). For example, 58 percent of the bomb-pulse samples were within 10 meters of a fault, and 75 percent were within 30 meters. We also found a strong correlation between the age of the water and the thickness of the nonwelded layer of Paintbrush tuffs that lies between the mountain top and both the potential repository and the exploratory tunnel. Pore water at the tunnel level was younger Holocene water where the layer is thinner and older Pleistocene water where it is thicker. Thus the nonwelded tuffs, which resemble spongy, hard-packed sand, apparently impede the downward flow of water. Only where a major fault intersected this tuff layer did any young bomb-pulse water reach the tunnel.

A simulation that assumes a constant water infiltration rate of 0.5 millimeter per year (mm/yr) shows general agreement with the chlorine-36 data (Figure 9). Bomb-pulse water moves rapidly through the upper layer of welded and highly fractured Tiva Canyon Tuff, but the nonwelded Paintbrush tuffs keep most water from percolating down into the Topopah Spring Tuff, which includes the tunnel and the repository site. In the northern half of the tunnel, most water in the Topopah Spring Tuff is at least 10,000 years old. In the southern half of the tunnel, where the Paintbrush tuffs are thinner, Holocene water as young as 1000 years old is found. Exceptions to this age pattern occur at major faults, where a small fraction (1 or 2 percent) of the water in fault zones at the repository level is bomb-pulse water that moved quickly to that depth.

Despite the general agreement between the simulation and chlorine data, however, there were some discrepancies in the details. In particular, the predicted bomb-pulse signal at the southern end of the tunnel did not appear in the pore-water samples. Nor does the simulation agree with the U.S. Geological Survey data, which indicate a spatially varying water infiltration rate. In fact, when we use the survey's infiltration rate in our simulations, predictions and experimental data are even more at odds. There is no flow of bomb-pulse water along fault fractures, and the distribution of the water's age is relatively uniform throughout the tunnel rather than changing as the thickness of the Paintbrush tuff layer changes.

However, our measurements of total chloride concentrations in pore water also differ from the survey results—for instance, infiltration rates toward the southern end of the tunnel appear to be lower than those deduced from the surface measurements. Lower infiltration rates would account for the fact that no bomb-pulse signal has been detected in faults in the southern half of the exploratory tunnel.

Thus the mere presence of major faults may not, by itself, result in fast water flow. Solutes can also travel by molecular diffusion into the surrounding rock matrix, where flow rates are apt to be orders of magnitude lower. A wide body of evidence, both theoretical and experimental, suggests that matrix diffusion is an important transport mechanism in fractured media. If the

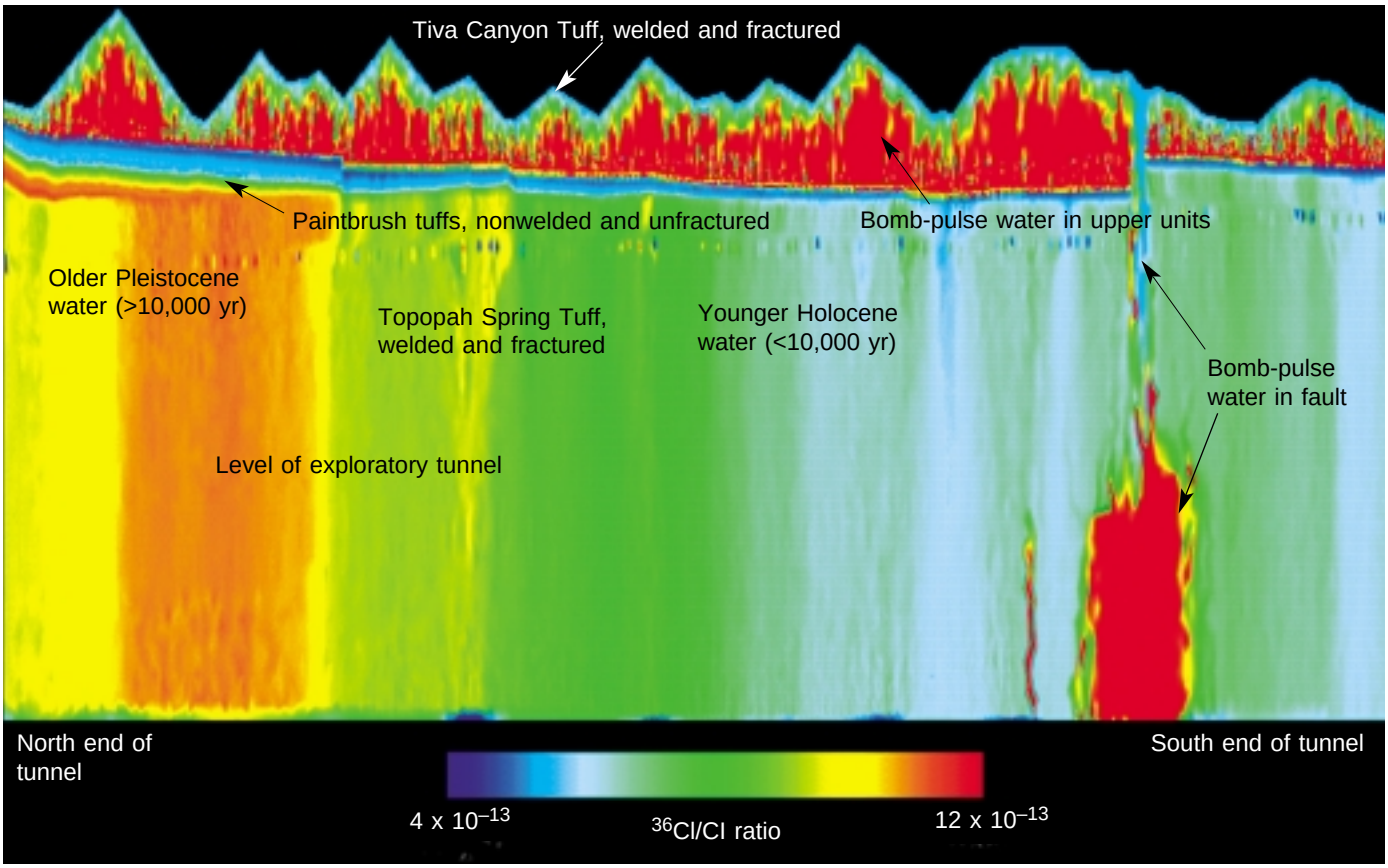

Figure 9. Simulation of $^{36}Cl/Cl$ Ratios in Yucca Mountain Groundwater

This simulation, which contains only one fault, generally agrees with analyses of the pore water in rock samples from the exploratory tunnel. Water moves rapidly through the upper Tiva Canyon layer of welded and highly fractured tuff. The next layer of nonwelded, unfractured, and porous Paintbrush tuffs, however, significantly impedes water flow. Thus, most of the young bomb-pulse water (red) remains in the Tiva Canyon Tuff. In the northern end, by the time water seeps through to the Topopah Spring Tuff—another welded, highly fractured layer—it is at least 10,000 years old (orange and yellow). Where the Paintbrush layer is thinner, the water is predominantly Holocene (blue and green). The exception occurs at a major fault, where a small amount of bomb-pulse water reaches the lower rock strata (red region on the right). Other simulations also predict bomb-pulse water at fault zones in the northern end of the tunnel.

infiltration rate is not high enough to support fracture flow, water will diffuse from fractures into the rock matrix, and downward flow may revert to slower percolation through the matrix.

It turns out that establishing the true infiltration rate, which ultimately governs the water flux through the unsaturated zone at Yucca Mountain, is much more important than showing the existence of fast-flow pathways. A neptunium atom cannot distinguish between water that is 50 years old and water that is 10,000 or 300,000 years old. Its transport toward the saturated zone will depend on the average net flux of water through the repository. As the flux of infiltrating water increases, rock saturation increases. As rock saturation increases, the capillary suction of the rock matrix decreases, reducing the matrix's ability to pull water out of fractures. Thus the potential for water flow in fractures increases.

Through a process that weighs the various surface, chloride, and chlorine-36 data and that reexamines the hydrologic properties of the various strata (i.e., their porosity, matrix permeability, and fracture density), we are moving closer to establishing a valid flux rate for assessing repository performance. At this point, we have found that using a spatially varying rate that averages 4 mm/yr yields reliable but conservative calculations. Ongoing field experiments at Busted Butte, discussed later, are helping us benchmark this parameter.

Laboratory transport tests indicate that fracture coatings also affect flow rates. These tests involved columns of Yucca Mountain tuff containing both natural and induced fractures. The natural fractures were coated with minerals that had been deposited over the eons; the induced fractures had no mineral coatings. By using a variety of tracers, we were able to sort out the

relative effects of flow through fractures, of matrix diffusion into rock micropores, and of sorption by fracture minerals. We found that because of sorption, neptunium arrived at the bottom of a column long after a nonsorbing tracer. Thus, minerals that appear to contribute insignificantly to sorption when they are present in trace quantities in the bulk rock may quite effectively retard transport when they are concentrated on fracture surfaces. Sensitivity studies are under way to assess the impact such sorptive minerals could have on radionuclide transport.

Unsaturated-Zone Transport

Our modeling studies of how effectively the natural barriers at Yucca Mountain will contain migrating waste radionuclides began with modeling travel times for neptunium through rock barriers in the unsaturated zone. To help us benchmark our modeling parameters, we are now conducting large-scale field experiments to measure the actual *in situ* transport properties of fractured rock. The experiments are under way at Busted Butte, about 8 kilometers southeast of the potential Yucca Mountain repository.

Unsaturated-Zone Simulations. We simulated neptunium transport from the repository to the water table with a site-scale model that accounts for speciation, sorption, diffusion, radioactive decay, repository heat, and both fracture and matrix flow. Figure 10 shows the results of a 2-D simulation for our base case, which used a spatially variable infiltration rate averaging 4 mm/yr and chemical data typical of Yucca Mountain groundwater: a pH of 8 with 150 milligrams per liter (mg/L) of bicarbonate, 125 mg/L of sodium, and 25 mg/L of calcium. The base case also assumed a repository design in which the density of waste canisters would lead to thermal loads high enough to boil water in the adjacent tunnel rock.

The first panel in Figure 10 shows the concentration of aqueous neptunium 2000 years after waste emplacement. By this time we assume that the waste canisters have begun to cool, that water has rewet the edges of the repository, and that some of the canisters have been breached by dripping water. Neptunium is dissolving and moving rapidly through the welded tuff below the repository via fracture flow. However, its migration is slowed significantly when it reaches the layer of Calico Hills nonwelded tuff (defined by the lower blue boundary), where matrix flow dominates.

The second panel, at 10,000 years, shows the transport plume after all repository rock has been rewet and all waste canisters are releasing neptunium. The third panel, at 50,000 years, shows the main neptunium plume reaching the water table. The aqueous neptunium concentrations are considerably reduced from those in the previous panel, mainly because of dilution with the percolating groundwater and sorption within the zeolitic tuffs in the Calico Hills layer. The final panel, also at 50,000 years, shows the concentration profile of immobile neptunium attached to zeolites. Comparison of the bottom two panels demonstrates that even though neptunium sorption onto zeolites is relatively small, it will still retard transport.

We have also carried out other base-case simulations to study the effect of varying assumptions for repository heat, water infiltration, and water chemistry. These studies indicate that the heat pulse from the decay of fission products in the waste does not significantly affect neptunium migration because the time scale of heat-pulse propagation is shorter than the time scales associated with neptunium release and migration. The major uncertainty in this conclusion is the possibility of rock/water interactions that permanently alter the rock's porosity, permeability, or mineralogy.

In regard to water chemistry, our studies show that the groundwater's pH and its calcium and sodium concentrations significantly affect how much the zeolitic and clay-bearing tuffs in the unsaturated zone retard neptunium transport. For example, a rise in pH to 9 decreases neptunium solubility, which results in slower releases from the repository. However, it also decreases the sorption of neptunium on zeolites, which leads to more rapid migration. The decrease in sorption would dominate, resulting in shorter travel times to the water table and higher peak concentrations for the radionuclide.

Our studies also show that small-scale variations in the site's chemical and hydrologic properties can affect neptunium transport and that such variations are strongly dependent on mineral distributions. In particular, zeolite distributions influence the flow patterns of percolating water and the sorption of many radionuclides. Where zeolitic abundance is low (less than 10 percent) and, thus, where neptunium sorption coefficients are low (K_d < 1 mL/g), the permeability is large enough for flow to be matrix dominated, causing significant retardation by diffusion despite the low K_d values. When our simulations account for such correlations, we find that neptunium transport is significantly retarded. Its transport is slowed even more when we account for the presence of smectite clays in the rock matrix.

Overall, our studies indicate that zeolitic sorption of neptunium in the unsaturated zone results in travel times that are much longer than 10,000 years, and thus the repository's primary regulatory goal can be met for this important limiting actinide. However, our modeling work is based on measurements from small-scale laboratory experiments that do not characterize the effects of larger geologic features such as faults and stratigraphic boundaries. To characterize the effects of these heterogeneities in the unsaturated zone, we are conducting large-scale field experiments at Busted Butte.

Busted Butte Field Studies. We chose Busted Butte because two major tuff layers that underlie the potential repository—Topopah Spring Tuff and

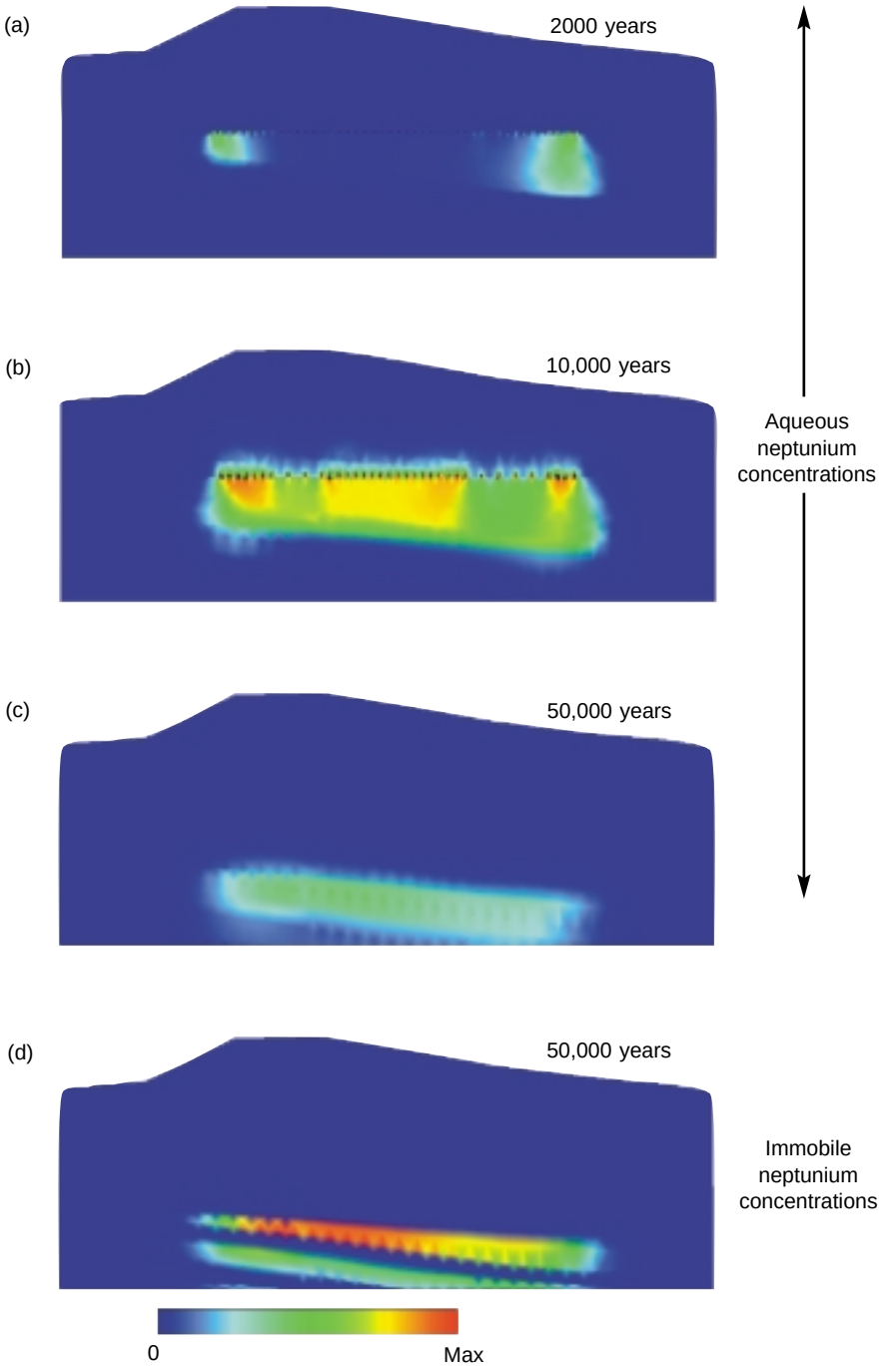

Figure 10. Simulated Neptunium Transport at Yucca Mountain

Our base-case analysis of neptunium transport at Yucca Mountain predicts that it will take the radionuclide 50,000 years to penetrate the mountain's rock barriers and reach the water table. The top three panels show the concentrations of aqueous neptunium as (a) the edges of the repository are rewet by water and some waste canisters begin to leak, (b) after all rock in the repository has been rewet and canisters throughout the repository are leaking, and (c) when the aqueous neptunium plume reaches the water table. Panel (d) shows the concentration of immobile neptunium sorbed onto zeolites at the same time that aqueous neptunium reaches the water table. Comparison of (c) and (d) demonstrates the effective role zeolites would play in retarding neptunium transport through sorption.

the Calico Hills Formation—are near the butte's surface and are readily accessible. These layers are actually distal extensions of the formations beneath the repository. The Busted Butte test site is 70 meters underground and is divided into several test blocks for a series of experiments (Figure 11). The idea is to inject aqueous tracers into the rock through horizontal boreholes, measure tracer migration, and then compare those measurements with our modeling predictions.

To mimic the behavior of neptunium and other radionuclides, we are injecting a mixture of both nonsorbing and reactive tracers and synthetic microsphere. Nonsorbing, or conservative, tracers (such as bromide) move with the aqueous phase and thus track

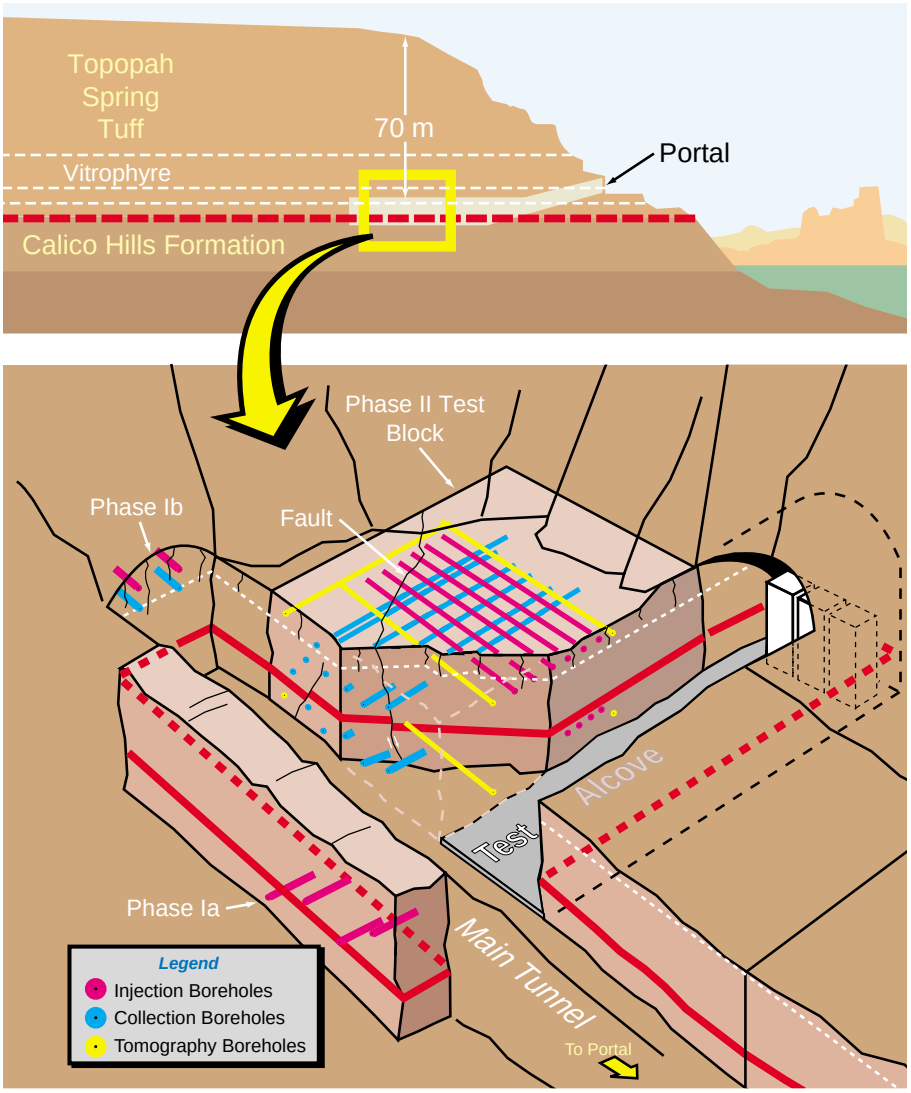

Figure 11. Busted Butte Field Test Site

Two of the repository's key unsaturated-zone tuff layers, the Topopah Spring Tuff and Calico Hills Formation, are only 70 m beneath the surface at Busted Butte. We are using these formations to measure tracer-solution transport times through large rock volumes. The site is divided into several test blocks, but the same general experimental procedure is being followed at each one: mixtures of tracers are injected through one set of horizontal boreholes and then detected either at parallel collection boreholes or by auger sampling and mineback. Comparing measured travel times for the tracers with our modeling predictions is helping us validate our transport models.

the movement of water and help determine the rock's hydrologic response. They capture processes involved in the migration of nonsorbing radionuclides such as technetium. Some of these tracers are ultraviolet fluorescent dyes (fluorescein and pyridone) that can be detected at a concentration of about 10 parts per million. Reactive tracers (such as lithium, manganese, nickel, cobalt, samarium, cerium, and fluorescent Rhodamine WT) diffuse into the rock matrix or sorb onto minerals and are used as analogs for sorbing actinides, such as neptunium. Finally, fluorescent polystyrene microspheres mimic the transport of colloids.

Some of the Busted Butte tests will validate our flow and transport models and provide new transport data for the hydrologic Calico Hills Formation. Other tests are located in the relatively low-permeability fractured rock at the base of the Topopah Spring Tuff to provide data on fracture/matrix interactions. Phase I tests, completed this past winter, involved simple, continuous, single-point tracer injection along horizontal boreholes 2 meters long. Although designed principally to test instrumentation, these tests are also providing valuable transport data.

Phase II tests, currently under way, are more sophisticated and use multi-point injection systems involving eight 8.5-meter-long boreholes, each with 9 injection points (Figure 12). The large Phase II test block (7 meters high, 10 meters wide, and 10 meters deep) allows us to study how large-scale heterogeneities will affect tracer migration. The tracers are dissolved in water that has the same composition as *in situ* pore water. Injection rates vary from 1 to 50 mL/h, which correspond to infiltration rates of 30 to 1500 mm/yr. The lowest injection rates correspond to the high end of infiltration rates for Yucca Mountain; the highest injection rates are designed to obtain data on greater travel distances within the experiments' 2-year time frame.

The Phase II tests are using three geophysical techniques (based on neutron assays, ground-penetrating radar, and electrical resistance measurements) to generate 2- and 3-D images of test-block saturation before and during the experiments.

Our first results came from the Phase Ib test, which was conducted at the base of the Topopah Spring Tuff. The test used a pair of injection/collection boreholes located near a vertical fracture and an injection rate of 10 mL/h (see Figure 11). The nonsorbing tracers began arriving at the collection boreholes, which are 28 centimeters beneath the injection points, about a month after injection. For the injection rate used, pure fracture flow would have resulted

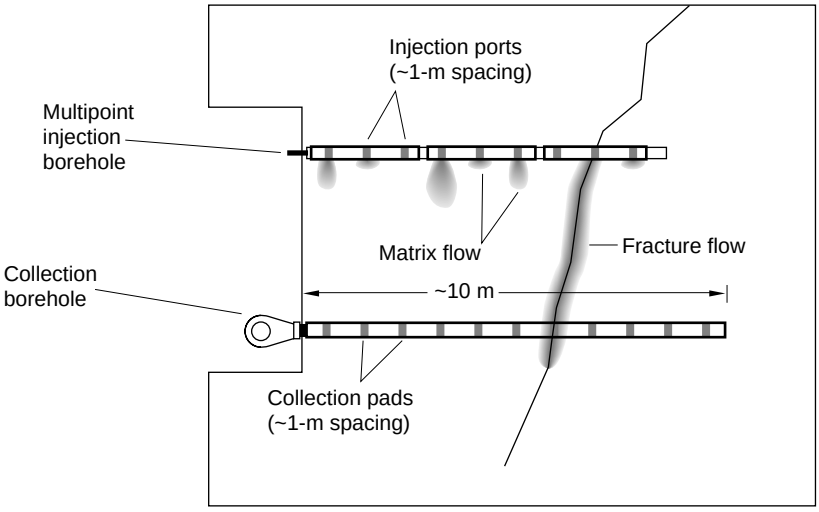

Figure 12. Multipoint Injection and Collection System for Phase II Tests

Multipoint injection and collection systems in the Phase II tests at Busted Butte are providing data on how large-scale heterogeneities, such as major fractures, affect tracer migration. The gray areas in this figure show hypothetical tracer movement, including rapid transport along a vertical fracture that intersects the injection and collection systems.

in travel times of hours to days. Although the concentration of tracers at the collection boreholes increased over the next couple of months, the tracers were detected at several collection pads on both sides of the fracture rather than just at the intercepting fracture plane.

These results indicate strong fracture/matrix interactions in the tuff, causing the tracers to diffuse from the fracture into the matrix and then move primarily by matrix diffusion. None of the reactive or colloidal tracers had reached the collection boreholes even six months after injection. Sample cores taken from the test block are currently being analyzed to determine how far these tracers traveled.

Our Phase Ia test was conducted in Calico Hills Formation tuff. In this test, we injected tracers from single points in each of four horizontal boreholes at two rates: 1 and 10 mL/h. After eight months of continuous injection, we began exposing vertical slices of the test block by mining into the rock face in stages to measure tracer migration (Figure 13). This was a "blind" test in that we used transport calculations to predict tracer movement before the mineback occurred. We are now comparing our predictions with results for the nonsorbing fluorescein tracer and are beginning to analyze samples for the reactive and colloidal tracers.

So far, it appears that strong capillary forces exist in the Calico Hills tuff

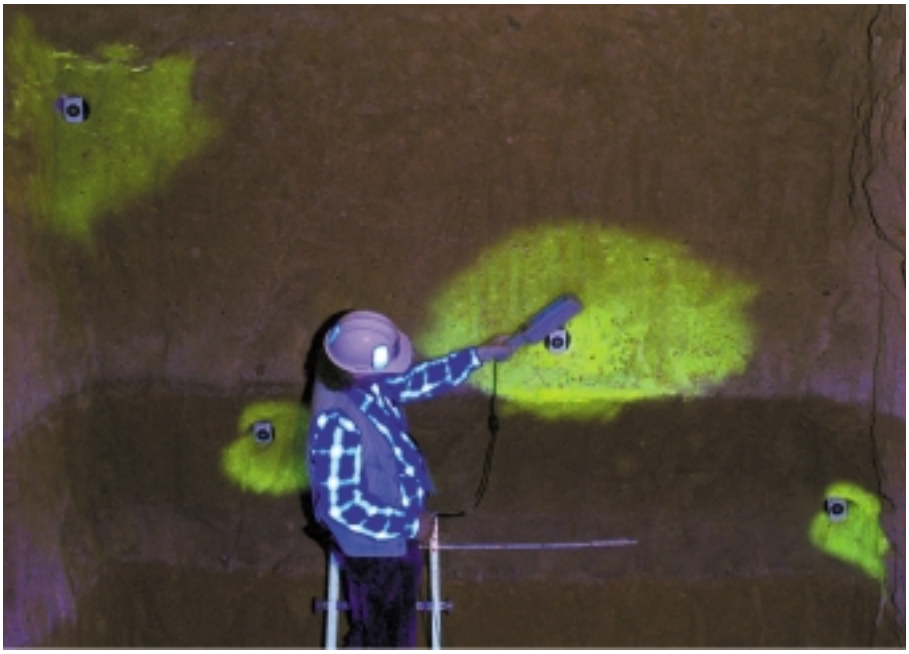

Figure 13. Mineback of Phase Ia Test in Calico Hills Tuff

In the Phase Ia test, a fluorescing tracer was injected into Calico Hills tuff from a single point in each of four horizontal boreholes (see test setup in Figure 11). After eight months of continuous injection, we exposed vertical slices of the test block by mining back the tuff in stages. In this photograph, the vertical plane passes through the injection points of the four boreholes. Ultraviolet light reveals the presence of the fluorescing tracer (yellow-green areas) around those points. The two larger fluorescent areas are a result of a 10-mL/h injection rate; the smaller areas, a 1-mL/h rate. Tracer movement appears to be mainly by diffusion through capillary flow. The upper-left borehole shows tracer diffusion in two perpendicular planes due to the presence of the left wall. The brighter yellow-green strip toward the bottom of the central fluorescent area reveals tracer accumulation at a boundary between two Calico Hills sublayers separated by 3 to 5 centimeters of silicified ash. Another boundary, this one rich in clay, passes horizontally above the upper-left borehole area, impeding upward capillary flow.

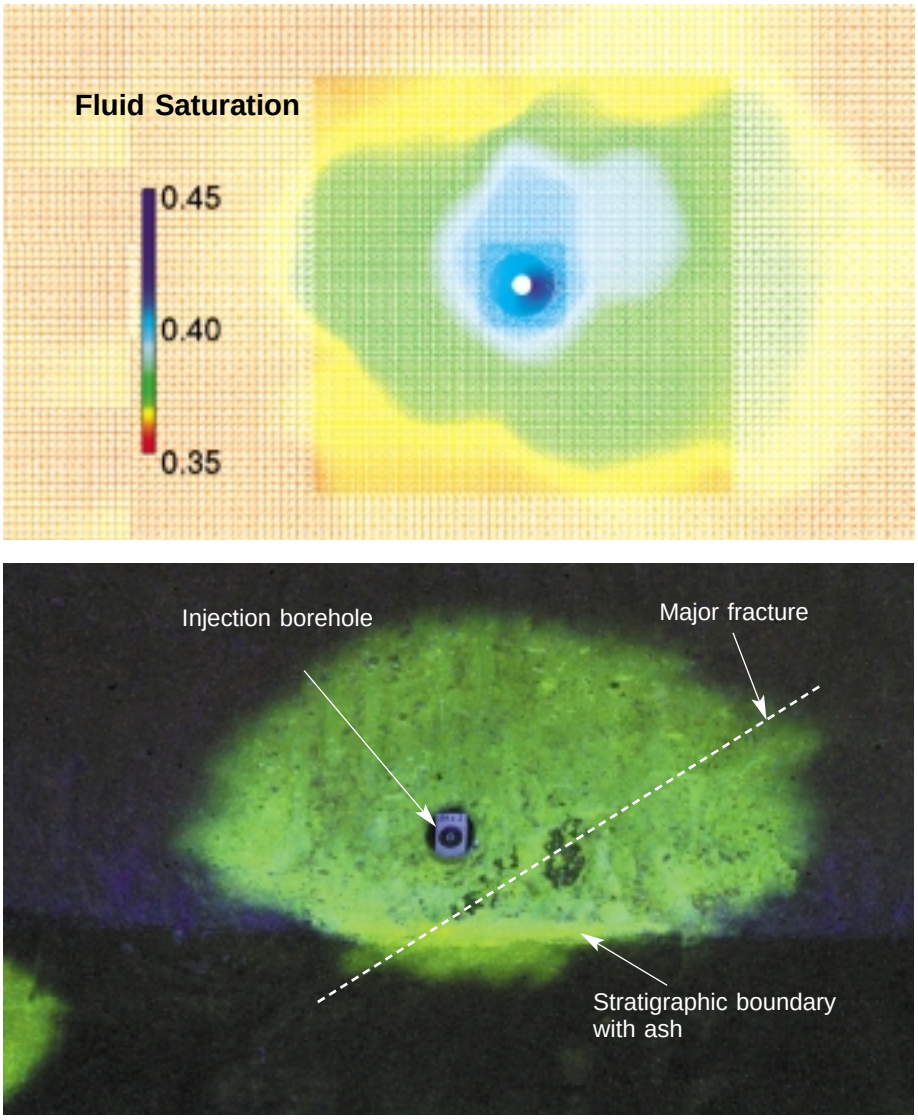

Figure 14. Capillary Flow in the Phase Ia Test vs Modeling Prediction
The bottom photograph, which focuses on the central fluorescent area in Figure 14, shows no appreciable tracer flow along a major fracture that passes diagonally just under the injection point. The fact that the tracer has not migrated significantly along this fracture indicates that the latter is not a fast-transport pathway but instead behaves as a large pore within a porous matrix. The photo also shows tracer accumulation (brighter yellow-green strip) at a layer of ash, which impedes tracer migration. Our modeling prediction for tracer movement (top graphic) agrees well with these test results. Its asymmetrical shape for tracer migration is accurate; what was missing in our model was any provision for the stratigraphic boundary formed by the thin layer of ash. We are now modifying our codes to include the impact of such heterogeneities.

that will modulate fracture flow from overlying rock layers, thereby damping pulses of infiltrating water and providing extensive contact between radionuclides and the rock matrix. Even when injection occurs next to a fracture, water is imbibed quickly into the surrounding matrix, and fracture flow is insignificant compared with matrix diffusion (Figure 14). Such results bode well for the performance of the repository's natural barriers: migration of water from the fractures into the rock matrix will lead to increased contact with sorbing minerals such as zeolites and clays. The combination of matrix diffusion and sorption will lengthen radionuclide travel times.

Where no heterogeneities (such as stratigraphic boundaries) are present, our nonsorbing-tracer predictions agree very well with measurements, capturing the asymmetric migration that results from injection through a single point on one side of the borehole. Likewise, our modeling predicts the predominance of capillary flow over fracture flow in the Calico Hills vitric tuffs (see Figure 14). However, nothing was included in the model to account for boundaries between tuff sublayers; these boundaries appear to locally retard tracer migration, whether the boundary lies above or below the borehole.

The Busted Butte experiments have also uncovered two uncertainties in our modeling. In particular, we are concerned about the adequacy of continuum models to describe transport in nonwelded tuff layers with high matrix permeabilities. Our dual-permeability models appear to be more accurate in representing the flow and transport processes of an unsaturated, fractured rock mass. Another problem is how to accurately characterize the transition from fracture flow to matrix flow at boundaries between tuff layers that have different hydrogeologic properties. When completed, the Phase II tests should help us resolve such uncertainties and bring our modeling even closer to realistically describing transport in the unsaturated zone at Yucca Mountain.

Saturated-Zone Transport

Although our unsaturated-zone modeling indicates that neptunium travel times to the water table will exceed 10,000 years, radionuclides will eventually reach it, releasing a radioactive plume into the saturated zone. The second part of our modeling

work, therefore, entailed simulating neptunium transport through the saturated zone and again benchmarking our modeling parameters with field experiments.

As in the unsaturated zone, groundwater will encounter both fractured and porous media in the saturated zone (Figure 15). In fractured media, groundwater may move relatively quickly through the fractures, but some water will move into progressively smaller cracks and pores, where advection, matrix diffusion, and sorption will help retard radionuclide transport. In porous media, such as alluvium, groundwater travel times will lengthen because the water must diffuse through the matrix rather than flow along fractures. Large-scale dispersion, or dilution, will also lower radionuclide concentrations in such media.

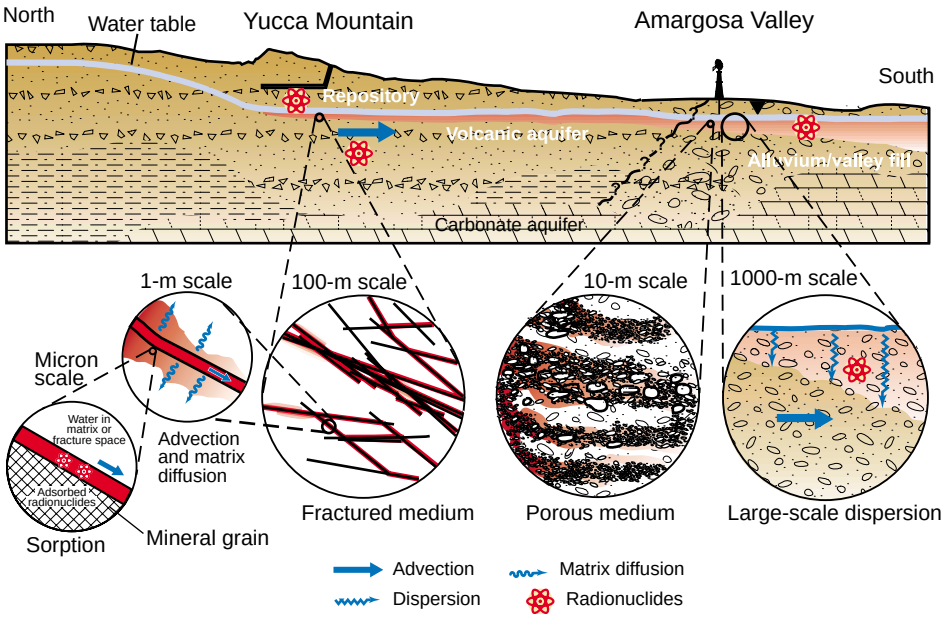

Figure 15. Conceptual Model of Radionuclide Transport in the Saturated Zone
A variety of factors will affect how quickly radionuclides travel through the saturated zone. As shown on the left, advection, matrix diffusion, and sorption will help retard radionuclide transport in fractured media. As shown on the right, porous media will slow advecive transport, and dispersion, or dilution, will lower the concentration of the radionuclides. Our saturated-zone simulations examine the interplay of all these factors.

Saturated-Zone Simulations. Transport simulations for the saturated zone were carried out to examine how long it would take for neptunium to reach the repository's site boundary, defined as 5 kilometers distant, and then travel another 15 kilometers to reach a point where it could be taken up in well water for Amargosa Valley. (This 20-kilometer point assumes that 10,000 years from now, the nearest valley population will be 10 kilometers closer to the mountain than it is today.) Our saturated-zone simulations examined how advective transport, diffusion into the rock matrix, dilution, and sorption would affect neptunium transport times.

The simulations indicate that the saturated zone could lower peak concentrations of radionuclides that bypass the unsaturated zone's natural barriers. Simply put, whenever a spike in elevated radionuclide flux reaches the water table, if the spike's duration is about the same as or less than the transport time of water through the saturated zone to the site boundary, then water in the aquifer will "dilute" the spike, both lowering its peak and stretching it out over a longer period of time. If, however, the radionuclide flux arrives at the water table over a long period of time, dilution will not occur—the flux will act as a constant source of radionuclides to the saturated zone. Thus, the saturated zone will provide a hedge against any failures of unsaturated-zone barriers that result in sharp influxes of radionuclides to the water table.

Initially, transport through the saturated zone will be in porous, fractured tuff. Our model thus includes both fracture flow and matrix diffusion. Inclusion of the latter slows neptunium travel times to the hypothetical site boundary from about one year for pure fracture flow to thousands of years. An important aspect of matrix diffusion is that it allows the radionuclides to come in contact with minerals in the surrounding rock that may adsorb them. As shown earlier in Figure 10, even small amounts of sorption have a large impact on radionuclide travel times and peak concentrations.

Figure 16 presents simulation results for a much more pessimistic waste-leakage scenario than that of our base case. In this simulation, we assume that the first waste canister fails at 1000 years and that neptunium leaks continuously over the next 30,000 years and then stops. The upper graph plots the arrival of neptunium at the water table; the lower graph plots neptunium transport through the saturated zone to the repository's site boundary for two cases: no sorption and weak sorption (an average K_d of 2 mL/g). Note that although sorption does not reduce the maximum concentration that arrives at the boundary, even weak sorption delays the initial arrival of neptunium by about 10,000 years.

We also examined the transport of radionuclides to a point 20 kilometers away from the repository. In these calculations, we had to account for flow that would include movement through highly porous alluvium (see Figure 15).

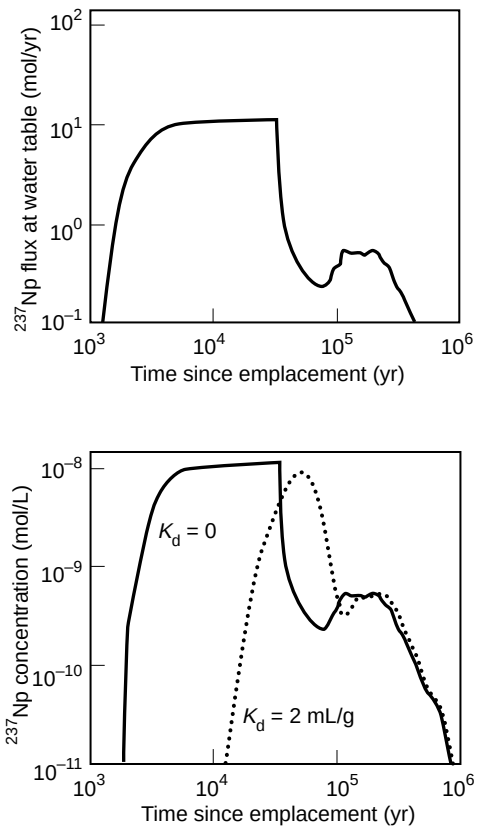

Figure 16. Neptunium Transport in the Saturated Zone

Even weak sorption significantly retards neptunium transport through the saturated zone. The two sets of graphs depict a worst-case scenario for waste leakage: the first waste canister fails at 1000 years, after which neptunium leaks continuously over the next 30,000 years. The upper graph shows the flux of neptunium-237 that crosses into the saturated zone. The lower graph shows resulting neptunium concentrations at the respository's site boundary, 5 km downstream, for two cases: no sorption (solid line) and weak sorption (dotted line).

As a result, neptunium travel times are considerably longer, with sorption in the alluvium adding from 10,000 to 50,000 years to them. As in our site-boundary calculations, sorption decreases the neptunium concentrations predicted to reach Amargosa Valley. Our calculations predict that after 100,000 years, neptunium concentrations in the valley would be no greater than 10 parts per trillion, which would pose a negligible health hazard. Thus, retardation from matrix diffusion and sorption and from the dilution effect noted above make the saturated zone an important component in the "defense in depth" provided by the mountain's natural barriers.

While encouraging, however, these calculations are not the final word. More experimental and modeling work must be done on the possibility of colloidal transport. Such transport would occur if radionuclides sorb not to stationary tuff but to particles so minute (1 nanometer to 1 micrometer in size) that they remain suspended in the groundwater and move with it. Colloidal transport became a concern when it was discovered that in just a few decades, a small amount of plutonium from an underground nuclear test had migrated more than a kilometer through the saturated zone, apparently by sorbing onto colloids. This transport process is discussed in the box on page 490.

Saturated-Zone Field Tests. To benchmark our modeling of the saturated zone, we conducted a series of field tests with tracers at a complex called the C-Wells. These wells are located about 2 kilometers southeast of the potential repository site and are drilled into fractured volcanic tuff. In terms of groundwater flow, they are directly downstream from the southern end of the repository.

In the C-Wells tests, we injected a variety of tracers into the saturated zone at one well and simultaneously pumped water out of another well about 30 meters away, establishing a recirculation loop between them. By adjusting packers in the injection well that sealed off selected intervals along its length, we were able to test transport through distinct stratigraphic layers having different hydraulic conductivities.

The tracers used were lithium bromide (composed of a small cation and small anion), pentafluorobenzate (PFBA, a large anion), and polystyrene microspheres (simulated colloids with a negative surface charge). The microspheres were tagged with a fluorescent dye so that they could be detected with flow cytometry. The bromide and PFBA are nonsorbing solutes with different diffusion coefficients, and lithium is a weakly sorbing solute. We conducted separate laboratory tests to characterize the sorption of lithium to C-Wells tuffs and the matrix diffusion coefficients of all tracers.

Figure 17 shows tracer concentrations at the second well as a function of time for one of our field tests. The most striking feature is the curves' bimodal shape. This shape is attributed to a relatively small fraction of the tracers moving quickly between the wells through densely welded, fractured tuff, while most of the tracers passed more slowly through partially welded, less fractured tuff. These results support the concept of dual-permeability that is incorporated into our simulation models: flow occurs primarily in fractures, but a large amount of near-stagnant water is present in the rock matrix to diffuse the tracers.

Looking more closely at the curves for the two nonsorbing solutes, we see that the PFBA peaks are slightly higher than the bromide peaks, that the second bromide peak occurs later than the corresponding PFBA peak, and that the bromide curve eventually crosses over the PFBA curve. These features are all consistent with greater matrix diffusion of the bromide, which is more diffusive than the PFBA.

The lithium curve is more attenuated than the curves for the two nonsorbing tracers, which indicates sorption. The attenuation in the first lithium peak is almost exclusively a lowering of the concentration with little or no delay in

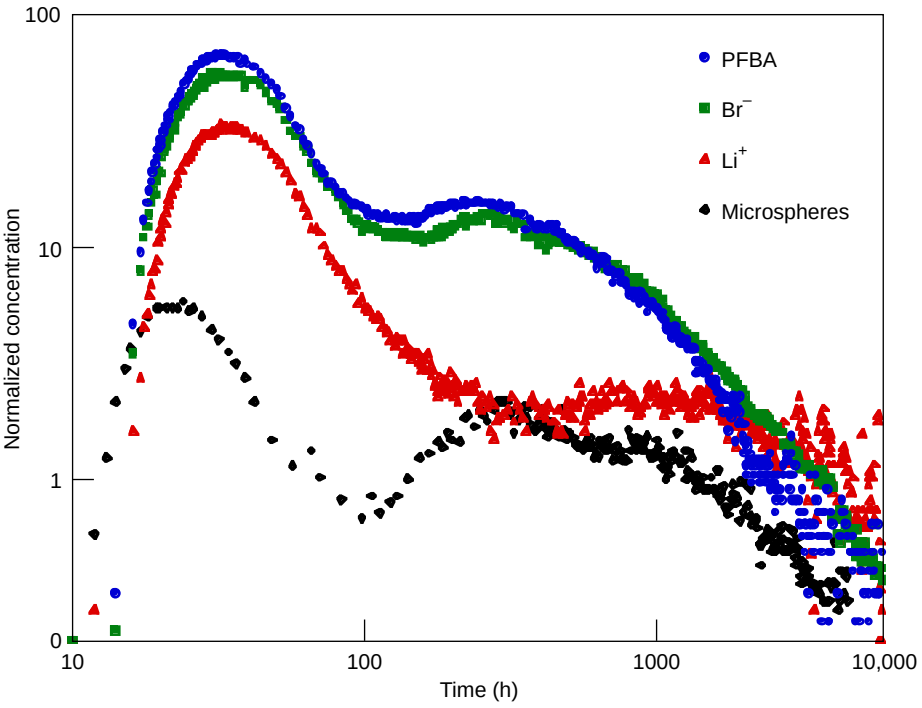

Figure 17. Saturated-Zone Field Tests at the C-Wells

A series of field tests at the C-Wells complex near the repository site helped benchmark our saturated-zone modeling parameters. The curves show the normalized concentrations of tracers injected at one well that were detected at a second well 30 m away. The data indicate multiple transport pathways for all tracers and validate matrix diffusion and sorption as important retardation mechanisms for radionuclide transport in the saturated zone.

arrival time. This reduction suggests that lithium diffuses into the matrix and is then sorbed. The attenuation in the second peak involves a clear time delay along with a dramatic lowering of concentration. This combination suggests lithium sorption in both the fractures and the matrix.

The microspheres reach the second well slightly earlier than the solutes, but their peaks are significantly attenuated. The attenuation implies that the rock matrix filters out a fraction of the microspheres, and the curve's bimodal shape suggests that two transport pathways are also available to the spheres. (These data and colloidal transport of radionuclides in general are discussed in the box on page 490.)

We were able to fit the curves of Figure 17 using a semianalytical, dual-porosity transport model, demonstrating that our simulations are consistent with field data. One important finding was that lithium sorption measured at the C-Wells was always equal to or greater than the sorption measured in laboratory tests. This correlation increases our confidence in laboratory measurements for radionuclide sorption onto Yucca Mountain tuffs.

Will the Repository Work?

Where have our extensive research and analysis brought us? Can a Yucca Mountain repository and its natural barriers safely isolate nuclear waste for 10,000 years? What radiation doses might the residents of Amargosa Valley receive 10,000 or 100,000 years from now, and when would those doses peak? The project's performance assessment team is beginning to answer such questions by combining the findings of the various laboratories studying the site. Input to its performance assessment includes calculations of waste-canister failure mechanisms and rates, of the effects of a volcanic eruption at the repository, of how radionuclides dissolve and are transported in groundwater, and of how these radionuclides would disperse in the biosphere once they reach Amargosa Valley.

The team's full report will not be published until 2001. However, estimates to date for two repository designs are that radiation doses to valley residents will be only 0.1 mrem/yr 10,000 years after the repository is closed and only 30 mrem/yr 100,000 years later. The latter dose is close to the EPA's regulatory limit of 20 mrem/yr. Radiation doses will reach a peak of 200 mrem/yr 300,000 years after the repository is closed. This peak, which is two-thirds of today's background dose from natural sources such as cosmic rays, radon, and radionuclides in the soil, results primarily from weakly sorbing neptunium and, later, from colloid-transported plutonium.

But again, these estimates are not the final word. For one, data are still being collected, such as from our ongoing Busted Butte tests. In addition, the performance estimates are based on very conservative assumptions, and our studies have shown radionuclide transport to be sensitive to a range of parameters. For instance, Figure 14 shows the impact strong capillary forces have on matrix diffusion, and Figure 16 shows the impact that even weak sorption in the saturated zone can have on transport times for neptunium. More laboratory and field data should yield more realistic assumptions. Finally, there is the challenge of predicting the performance of natural and engineered barriers over geologic time scales.

As the assessment team points out, "whether these calculated annual doses will actually occur cannot be physically demonstrated or scientifically proven. The performance of a repository over

such long periods—longer than recorded human history—cannot be tested in the same way that the performance of an airplane, for example, can be tested." *Proof* of the repository's viability cannot be given in the ordinary sense of the word. However, the project's iterative process of experimental measurements, modeling calculations, and analysis is moving us ever closer to a more accurate portrayal of repository performance and hence to greater confidence in our predictions.

Epilogue

We may pause at this point and ask ourselves what Yucca Mountain will look like 10,000 years from now. Will black-tailed jackrabbits and desert collared lizards still scurry across a brown, nondescript ridge, hiding behind the occasional Yucca plant? Or will the climate have changed, making the mountain greener, perhaps covered with a dense juniper forest? If a solitary hiker, reaching the ridge top, comes across a monument inscribed with hieroglyphics, will she be able to decipher the message? Will she realize that beneath her feet lies the entombed waste of the 20th century's nuclear age?

Perhaps in her pack she'll carry a faded graph handed down over the ages from an ancient ancestor, the computer modeler. The graph will have been passed on, parent to offspring, for generation upon generation. According to the graph, by her time in the 121st century, the total dose for all pathways and from all radionuclides should still be barely 0.1 mrem/yr.

Perhaps in her backpack she'll also carry the instruments needed to check her ancestor's prediction. After examining the mountain for signs of erosion, new earthquake faults, or volcanism and after checking the meteorological station for annual rainfall, perhaps she'll return to her solar-powered vehicle and drive over to Amargosa Valley. If farmers there are still growing crops, what will she find when she pulls out her mini-mass spectrometer and measures the concentration of neptunium in the their irrigation water? Will she grumble at the stupidity of her ancestors or smile at their wisdom? According to the statistical analysis given in the faded graph she's carrying, there's a 90 percent chance she'll smile. ■

Acknowledgments

The research by Los Alamos on Yucca Mountain has so many facets and is so extensive that anyone close to the project can quickly lose the general reader in massive amounts of detail. We would like to acknowledge the difficult and important work of Judy Prono on this article. She brought the right amount of objectivity to the task, asking various investigators to explain or amplify on the material until she gradually, paragraph by paragraph, section by section, made the article much more accessible to a wide audience.

In this same vein, the article represents the work of many individuals at the Laboratory over several decades. The people listed at the beginning of the article or pictured at the end are only representative of the entire effort. Others whose work also contributed the Yucca Mountain Project include Kay Birdsell, Kathy Bower, Dave Broxton, Katherine Campbell, Dave Clark, Jim Conca, Bruce Crowe, Dave Curtis, John Czarnecki, Zora Dash, Clarence Duffy, Ned Elkins, Claudia Faunt, Dick Herbst, Larry Hersman, Stephen Kung, Ed Kwicklis, Ningpin Lu, Arend Meijer, Dave Morris, Mary Neu, Heino Nitsche, Ted Norris, Don Oakley, Jeffrey Roach, Robert Rundberg, Betty Strietelmeier, Kim Thomas, Joe Thompson, Bryan Travis, Lynn Trease, Peng-Hsiang Tseng, Greg Valentine, Kurt Wolfsberg, and Laura Wolfsberg. I would especially like to thank Chuck Harrington, Frank Perry, Tom Hirons, Ken Eggert, and Wes Meyers for supporting the work of assembling this article, critiquing early drafts, or providing helpful material on the history of Yucca Mountain.

Further Reading

CRWMS M&O (Civilian Radioactive Waste Management System, Management and Operating) Contractor. 2000. "Analysis of Geochemical Data for the Unsaturated Zone (U0085)." CRWMS M&O report ANL-NBS-HS-000017.

——— 2000. "Calibration of the Site-Scale Saturated Zone Flow Model." CRWMS M&O report MDL-NBS-HS-000011.

——— 2000. "Particle Tracking Model and Abstraction of Transport Processes." CRWMS M&O report ANL-NBS-HS-000026.

——— 2000. "Saturated Zone Transport Methodology and Transport Component Integration." CRWMS M&O report ANL-NBS-HS-000036.

——— 2000. "Unsaturated Zone and Saturated Zone Transport Properties (U0100)." CRWMS M&O report ANL-NBS-HS-000019.

New Questions Plague Nuclear Waste Storage Plan. 1999. *New York Times*. August 10 issue.

Office of Civilian Radioactive Waste Management. 1999. "Viability Assessment of a Repository at Yucca Mountain" (December). U.S. Department of Energy report DOE/RW-0508. (The full report is available on the World Wide Web at http://www.ymp.gov/va.htm)area

Roger Eckhardt has a Ph.D. in physical chemistry from the University of Washington but has spent a great deal of his professional life involved with science education and science writing. Most recently, he has been helping to compile and write the voluminous documents that describe the scientific work being carried out at Los Alamos for the Yucca Mountain Project.

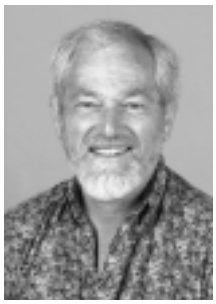

Principal Los Alamos Contributors to the Yucca Mountain Project

Julie A. Canepa
Former project manager. Currently, program manager of LANL Environmental Restoration Project.

Paul R. Dixon
Project manager.

David L. Bish
mineralogy of Yucca Mountain tuffs.

Gilles Y. Bussod
Busted Butte unsaturated-zone transport test.

James W. Carey
Mineralogical modeling of Yucca Mountain.

Steve J. Chipera
X-ray diffraction mineralogy.

June T. Fabryka-Martin
Yucca Mountain chlorine-36 studies.

Schön S. Levy
Alteration history of volcanic rocks at Yucca Mountain.

Maureen McGraw
Modeling of colloid-facilitated transport.

Mark T. Peters
Yucca Mountain testing, including the Exploratory Studies Facility and Busted Butte experiments.

Paul W. Reimus
C-Wells studies at Yucca Mountain.

Bruce A. Robinson
Modeling of flow and transport in the unsaturated and saturated zones.

Wolfgang H. Runde
Actinide solubility and speciation at Yucca Mountain.

Wendy E. Soll
Modeling of Busted Butte hydrology.

Carleton D. Tait
Actinide solubility and speciation in Yucca Mountain groundwaters.

Inés Triay
Yucca Mountain geochemistry, including sorption, diffusion, and transport in tuffs. Currently, DOE manager for WIPP.

Jake Turin
Field hydrology for Busted Butte.

David T. Vaniman
Igneous petrology and mineralogical analysis of Yucca Mountain tuffs.

Andrew V. Wolfsberg
Modeling of colloids and chlorine-36 transport.

George A. Zyvoloski
Modeling of flow and transport in the saturated zone.